balt3/zbc-bc/zbc-bc/zbc04409/zbc9087-09z xppws S=1 21/8/09 8:31 4/Color Figure(s) F2,4 ARTNO: M109.038802

observation of KLRG1 binding to ^{15}N-labeled EC-D1D2, a series of ^{1}H-^{15}N heteronuclear sequential quantum correlation (HSQC) spectra at 1:0 (EC-D1D2/KLRG1, 70 μM:0 μM), 1:0.5 (70 μM:35 μM), 1:1 (70 μM:70 μM), and 1:2 (70 μM:140 μM) ratios were measured at 25 °C. All HSQC spectra were measured at 25 °C and collected on 600-MHz spectrometers (Bruker) equipped with cryoprobes. The collected data were analyzed by NMRView. Chemical shift changes were defined by the formula, $((\delta_{H})^2 + (\delta_{C}/5)^2)/2)^{1/2}$ (19).

Mutant Preparation—Alanine-scanning and D90K mutagenesis of EC-D1D2 were performed using a QuikChange (Stratagene) kit with pET15bEC-D1D2(His10Xa) as the template. All of the EC-D1D2 mutants accumulated as soluble protein and purified in the same manner as EC-D1D2(His10Xa). SPR experiments for all mutants were performed in HBS-P buffer with 3 mM EDTA.

Cell Lines and Reagents—Mouse thymoma cell line BW5147 and mouse NK cell line NK 03 expressing KLRG1, KLRG1-NK03, were prepared as described previously (5). The retrovirus vector, pMXs-IRES-GFP, and retrovirus packaging cell line, Plat-E, were kindly provided by T. Kitamura (University of Tokyo).

Culture supernatant from anti-mouse E-cadherin monoclonal antibody ECCD-2 hybridoma cells was kindly provided by M. Takeichi (Institute of Physical and Chemical Research CDB, Hyogo, Japan) and was used to assess E-cadherin expression. Goat F(ab')$_2$ fragment of anti-mouse IgG(H+L)-phycoerythrin (PE) was purchased from Beckman Coulter.

Expression of E-cadherin on BW5147 Cells by Retroviral Transduction—DNA encoding the entire extracellular region of wild-type and mutant *M. musculus* E-cadherin was ligated into the pMXs-IRES-GFP vector using XhoI and NotI restriction enzyme sites to produce pMXs-WT mEC-IRES-GFP. These vectors were transfected into retrovirus packaging Plat-E cells, using Lipofectamine 2000 reagent (Invitrogen). Culture supernatants containing retrovirus were used to transduce BW5147 cells. BW5147 cells were stained with anti-mouse E-cadherin antibody (ECCD-2) and goat F(ab')$_2$ fragment anti-mouse IgG(H+L)-PE to confirm the expression of E-cadherin. Data were acquired with a FACSCalibur system (BD Biosciences) and analyzed with FlowJo software (TreeStar, Inc.).

KLRG1 Tetramer Binding Assay—KLRG1 tetramer was formed by incubating soluble biotinylated KLRG1 with PE-coupled streptavidin, as previously reported (20). The concentration of KLRG1 tetramer used in the binding studies was 20 μg/ml. BW5147 cells expressing E-cadherin were incubated with KLRG1 tetramer or PE-coupled streptavidin in Hanks' solution 2 (Nissui Pharmaceuticals) containing 0.1% bovine serum albumin and 0.1% NaN_3 (fluorescence-activated cell sorting buffer) and were then analyzed by FACSCalibur.

KLRG1 Reporter Assay—The KLRG1 reporter cell line was established as described previously (5). The reporter cells were stimulated by target cells expressing E-cadherin for 16 h at 37 °C in 5% CO_2, and then accumulated β-galactosidase activity was determined by a colorimetric assay using chlorophenol red-β-D-galactopyranoside (Wako Pure Chemicals) as substrate.

Killing Assay—The cytotoxicity of KLRG1-expressing NK03 cells against target cells expressing E-cadherin was examined using 6-carboxyl-succinimidyl-fluorescein ester (Dojindo) and 7-amino-actinomycin (Sigma). First, BW5147 cells expressing E-cadherin were incubated with 6 μM 6-carboxyl-succinimidyl-fluorescein ester at room temperature for 5 min in the dark. Afterward, 6-carboxyl-succinimidyl-fluorescein ester-labeled target cells were incubated with effector KLRG1-expressing NK03 cells in the presence or absence of anti-KLRG1 3D4 F(ab')$_2$ in a CO_2 incubator for 6 h in the dark. The expression of E-cadherin protected the target cells from killing by KLRG1-expressing NK03 cells, and the protection was reversed by inhibiting the KLRG1-E-cadherin interaction with anti-KLRG1 3D4 F(ab')$_2$. Then 1 μg/ml 7-amino-actinomycin was added to the reaction solution, and cells were incubated on ice for 15 min. Data were collected using the FACSCalibur system and analyzed on FlowJo.

RESULTS

Preparation of Recombinant Proteins—N-terminal domains 1 and 2 of *M. musculus* E-cadherin (residues 1–221) with a His_{10} tag, a spacer sequence, and a Factor Xa recognition site at the N terminus were expressed in *E. coli* either as a soluble protein or inclusion bodies. The soluble protein was purified using Ni^{2+}-nitrilotriacetic acid chromatography, and the inclusion bodies were refolded by the standard dilution method. For both proteins, the extra N-terminal amino acids were removed with Factor Xa, resulting in the authentic N-terminal sequence (Asp^1-Trp^2-Val^3-) (designated as EC-D1D2). EC-D1D2 was further purified by ion exchange chromatography. A final yield of 2–4 mg of purified EC-D1D2 was obtained from 1 liter of culture. N-terminal domains 2 and 3 of *M. musculus* E-cadherin (designated as EC-D2D3; residues 109–332) was also produced as inclusion bodies in *E. coli* and refolded by the standard dilution method. The refolded protein was purified by gel filtration chromatography.

Next, the extracellular region of *M. musculus* KLRG1 (residues 72–188) was expressed in *E. coli* as inclusion bodies. KLRG1 was refolded by the dilution method, in a similar manner as E-cadherin. The refolded protein was purified by gel filtration chromatography (Fig. 1, *A* and *B*), and the final yield was 1 mg of KLRG1 from 1 liter of culture.

Surface Plasmon Resonance Analysis of KLRG1-E-cadherin Binding—To clarify the molecular interaction between KLRG1 and E-cadherin, we performed SPR analysis, using recombinant E-cadherins EC-D1D2 and EC-D2D3. Recombinant E-cadherin variants EC-D1D2 and EC-D2D3 were injected over the flow cells, in which biotinylated KLRG1 had been immobilized at a level of 1,000 response units. As a negative control, biotinylated bovine serum albumin was immobilized on one of the flow cells, at a level similar to that of KLRG1. The response derived from the negative control was subtracted from each response derived from the recombinant E-cadherins. Fig. 1, *C* and *D*, shows the conventional plots of these binding data. In accordance with recent results showing that the deletion of either domain 1 or 2 abolished reactivity in KLRG1 reporter cell assays (18), Fig. 1*C* indicates that KLRG1 can bind to domains 1 and 2 of E-cadherin (EC-D1D2) but not to domains 2 and 3 (EC-D2D3). The KLRG1-EC-D1D2 interaction conforms to a simple 1:1 (Langmuir) binding model, and its dissociation con-

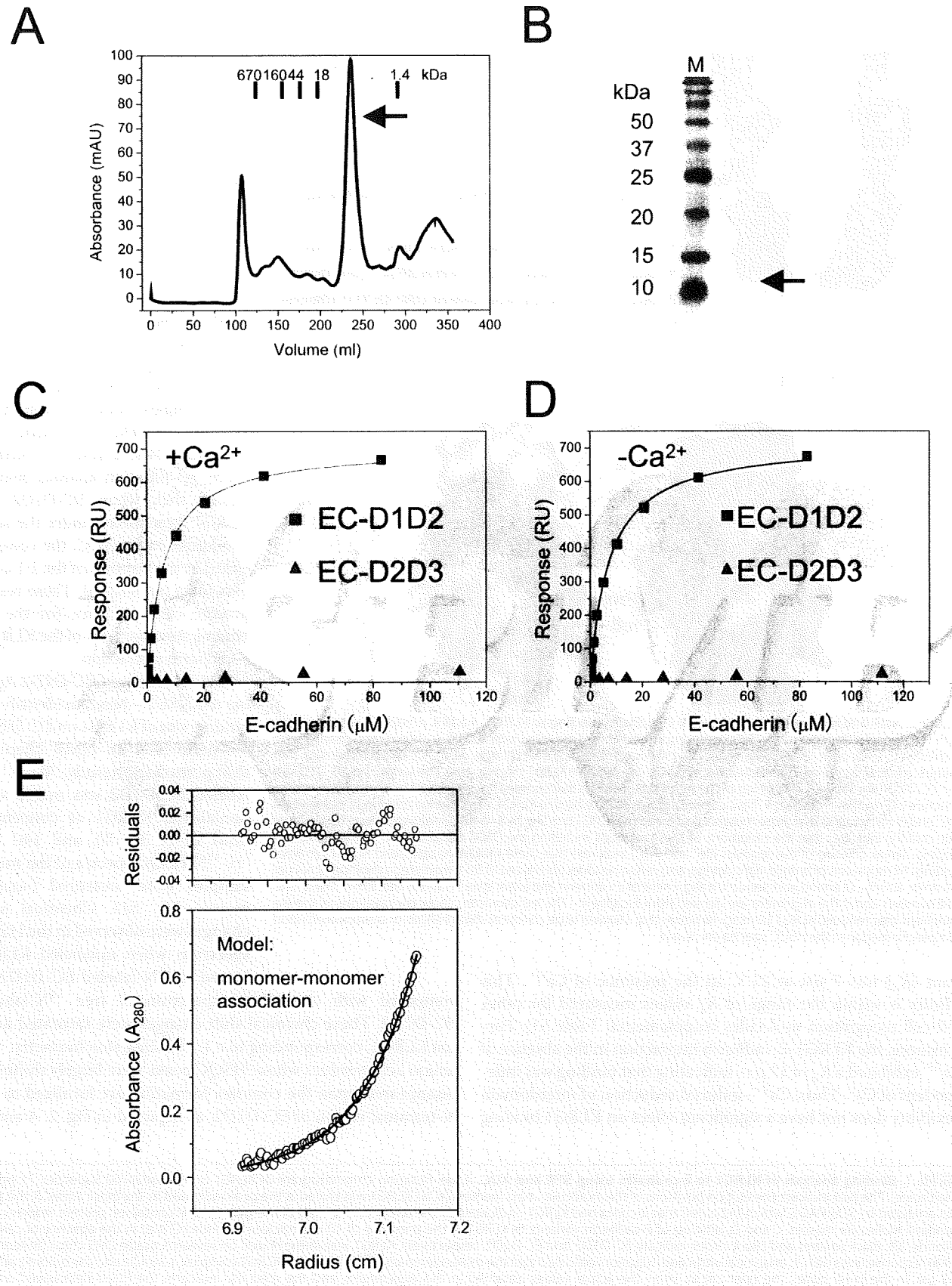
A
67
016
044
18
1.4 kDa
Absorbance (mAU)
Volume (ml)
B
M
kDa
50
37
25
20
15
10
C
+Ca2+
EC-D1D2
EC-D2D3
Response (RU)
E-cadherin (μM)
D
-Ca2+
EC-D1D2
EC-D2D3
Response (RU)
E-cadherin (μM)
E
Residuals
Model:
monomer-monomer
association
Absorbance (A280)
Radius (cm)

balt3/zbc-bc/zbc04409/zbc9087-09z xppws S=1 21/8/09 8:31 4/Color Figure(s) F2,4 ARTNO: M109.038802

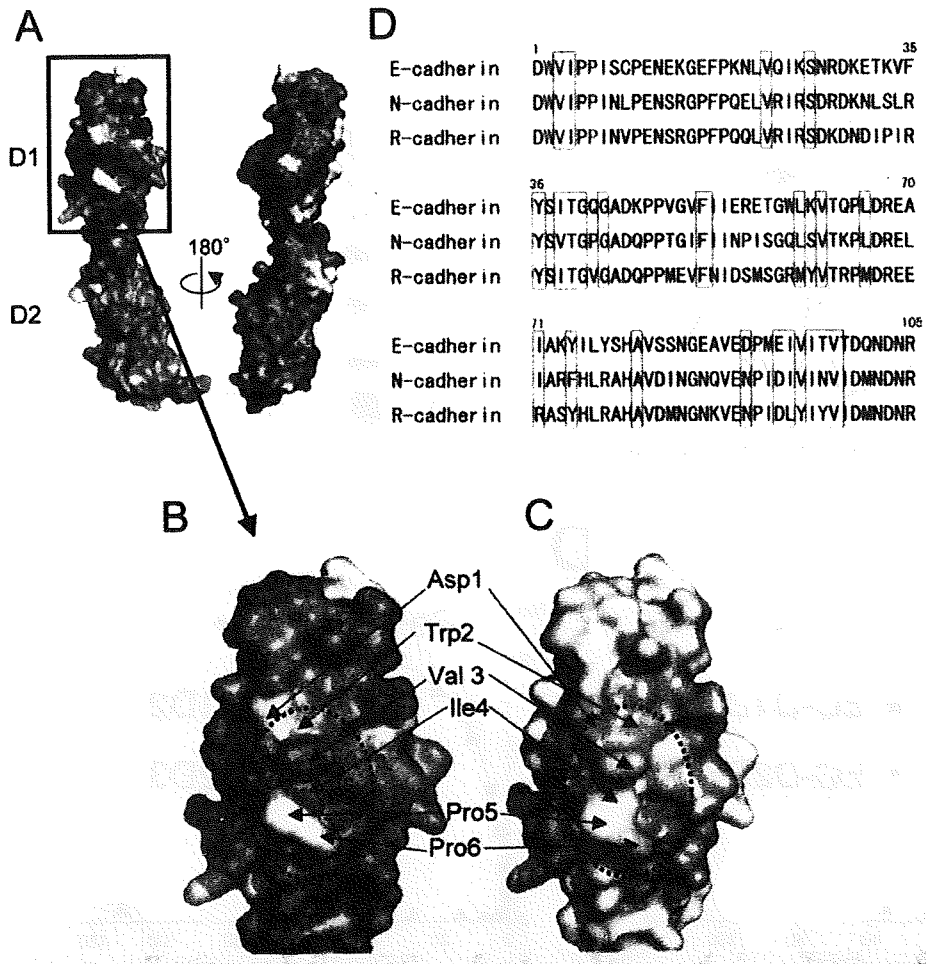

FIGURE 2. **NMR and mutagenesis analyses of E-cadherin binding to KLRG1.** *A* and *B*, a map of the amino acids with HSQC peaks that shifted or disappeared upon complex formation with KLRG1 is shown (*red*, disappeared; *purple* (Tyr[36], *small open circle* to the *right* of *A*), >0.06ppm chemical shift change; *green*, <0.06 ppm chemical shift change; *white*, unassigned). The *dotted line* indicates the putative KLRG1 binding area. The surfaces of EC-D1D2 (*A*) and EC-D1 (*B*) are shown. *C*, mapping of the significant residues that showed no or reduced binding affinity on the structure of E-cadherin domain 1. Trp2, *colored orange*, did not bind to KLRG1. *Light orange coloring* of the residues (Val[3] and Pro[6]) indicates that these mutations reduced the KLRG1 binding by 5–6-fold, relative to the wild type. *Light blue coloring* indicates that the mutations of these residues, including the D90K mutation, did not affect KLRG1 binding. *Yellow coloring* of the residues (Ile[4] and Pro[5]) indicates that these mutations abolished KLRG1 tetramer binding. All mutations of *orange*, *light orange*, and *yellow* residues abrogated KLRG1-mediated inhibition of NK cell cytotoxic activity. *D*, amino acid sequence alignment of E-cadherin and other type I classical cadherins. The amino acid *numbers above* the alignment are derived from E-cadherin. The *red characters* show the positions of the Ala mutations that reduced KLRG1 binding. Residues that showed large chemical shift changes or disappeared upon complex formation in the HSQC spectra are *boxed*.

stant (K_d) was 7 μM at 25 °C in the presence of Ca^{2+}. This affinity is within the range of K_d values measured for other cell-cell recognition molecules (supplemental Table S1). Furthermore, the KLRG1-E-cadherin interaction in the absence of Ca^{2+} exhibited a K_d of 12 μM, indicating that binding was independent of Ca^2. Thus, Ca^{2+}-induced reduction of interdomain flexibility does not have a significant effect on KLRG1 binding (Fig. 1, *C* and *D*; summarized in supplemental Table S1). These results imply that KLRG1 binding is dependent on the N-terminal domain of E-cadherin.

Characterization of the EC-D1D2-KLRG1 Complex—The SPR data indicated that the EC-D1D2-KLRG1 interaction occurs at 1:1 stoichiometry. To confirm this, we performed AUC. Solutions of EC-D1D2 and KLRG1 were mixed at a molar ratio of 1:1. The experimental data fit well to the monomer-monomer association model (Fig. 1*E*). The estimated molecular mass of the EC-D1D2-KLRG1 complex was 36 kDa, which corresponds to the molecular mass of a complex between monomeric KLRG1 (13 kDa) and monomeric EC-D1D2 (24 kDa) (Fig. 1*E*). Furthermore, gel filtration analysis demonstrated that, when EC-D1D2 and KLRG1 were mixed under the same conditions as for AUC, the complex eluted at the position of the 1:1 complex (data not shown). These results provide clear evidence for the 1:1 binding stoichiometry of the KLRG1-E-cadherin interaction.

NMR Analysis of EC-D1D2 Binding to KLRG1—Next, to identify the binding site of KLRG1 on EC-D1D2, we performed an NMR chemical shift perturbation study. 70 μM ^{15}N-labeled EC-D1D2 was mixed with nonlabeled KLRG1 at concentrations of 0, 35, 70, and 140 μM. ^{1}H-^{15}N HSQC spectra of the mixed samples were measured (supplemental Fig. S1). Chemical shift changes were observed in the HSQC spectrum when unlabeled KLRG1 bound to ^{15}N-labeled EC-D1D2, as compared with the HSQC spectrum of free ^{15}N-labeled EC-D1D2. These chemical shift changes were saturated at 70 μM KLRG1, corresponding to a 1:1 binding stoichiometry. The amino acid residues whose HSQC peaks were largely shifted or disappeared upon the complex formation are localized to the N-terminal region of EC-D1D2, as depicted in Fig. 2, *A* and *B*.

FIGURE 1. **Binding analysis of KLRG1 to E-cadherin using SPR and AUC.** *A*, gel filtration chromatogram of KLRG1 on HiLoad26/60 Superdex 75 pg (GE Healthcare). The *bars* indicate the elution positions of the molecular mass markers (kDa). KLRG1 was eluted at the peak indicated by the *black arrow*. *B*, this peak was analyzed by SDS-PAGE, which indicated that it contained KLRG1 (indicated by the *arrow* on the *right* of the gel). *Lane M* contained protein markers with standard molecular masses. *C* and *D*, binding of E-cadherin variants to KLRG1 in the presence of 10 mM calcium chloride (*C*) and in the absence of calcium chloride (*D*). *Black squares* and *black circles* indicate EC-D1D2 and EC-D2D3, respectively. KLRG1 was immobilized on research grade CM5 chips (BIAcore) at 1,000 response units (*RU*). *E*, analytical ultracentrifugation indicated that the molecular mass of the EC-D1D2-KLRG1 complex is 36 kDa and the binding affinity is 9 μM. In the *lower panel*, the *open circles* show the actual values obtained in this experiment, and the *solid line* indicates the fitted data based on the monomer-monomer binding model. In the *upper panel*, the residuals derived from the fitted data are shown.

TABLE 1

SPR study of KLRG1 binding to wild-type and mutant E-cadherin

The ligand was KLRG1, and the analytes were EC-D1D2 mutants, including D90K. The values are means ± range derived from two experiments. NB, no binding.

Analytes	K_d (25 °C)	Analytes	K_d (25 °C)
	μM		μM
Wild type	12 ± 3.0	K73A	5.5 ± 0.7
D1A	19 ± 0.0	I75A	8.0 ± 0.0
W2A	NB	Y77A	22 ± 0.0
V3A	66 ± 2.1	E89A	30 ± 0.7
P6A	86 ± 9.2	D90K	20 ± 2.1
N20A	14 ± 0.7	P91A	8.6 ± 0.2
F35A	7.8 ± 0.1	E93A	24 ± 2.8
S37A	6.2 ± 0.3	V95A	22 ± 0.0
T39A	8.8 ± 0.3	T97A	19 ± 0.7
Q64A	13 ± 0.7		

This result indicates that KLRG1 can recognize the N-terminal region of EC-D1D2. The opposite face of the N-terminal region did not have any residues that showed large chemical shift changes (Fig. 2*A*).

Mutagenesis Mapping of the KLRG1 Binding Site on E-cadherin by Tetramer Staining and Reporter Cell Assays—To confirm the results of the NMR binding study, alanine-scanning mutagenesis was performed. The mutants of EC-D1D2, shown in Table 1, were prepared as described under "Experimental Procedures." SPR analysis using these mutants showed that the W2A mutant cannot bind to KLRG1. In addition, both the V3A and P6A mutants showed significantly reduced KLRG1 binding. All of these amino acids are in the N-terminal region of E-cadherin (Fig. 2, *C* and *D*), consistent with the results of the NMR analysis. The other mutants, including the D90K mutant, bound to KLRG1 at levels comparable that of the wild-type protein. The mutagenesis data are summarized in Table 1.

To further examine the KLRG1 binding site on the N-terminal region of E-cadherin, KLRG1 tetramer binding to wild type or a series of mutant E-cadherins (D1A, W2A, V3A, I4A, and P5A) expressed on the cell surface was examined by flow cytometry (Fig. 3*A*). BW5147 cells expressing wild-type or mutant E-cadherin were generated by retroviral transduction, and E-cadherin expression was confirmed by anti-E-cadherin staining with monoclonal antibody, ECCD2, as shown in supplemental Fig. S2. PE-conjugated KLRG1 tetramer was prepared as described under "Experimental Procedures." The W2A, V3A, I4A, and P5A mutants failed to bind the KLRG1 tetramer. These data indicate that KLRG1 recognizes a relatively large area of the N-terminal region of E-cadherin that is responsible for homophilic association, supporting the idea that KLRG1 can only bind to monomeric E-cadherin. Interestingly, the D1A mutant E-cadherin bound to the KLRG1 tetramer at levels comparable with that of wild type (Fig. 3*A*).

We next performed KLRG1 reporter cell assays using the KLRG1-expressing cell line BWZ.muKLRG1 and BW5147 cells expressing either wild-type or mutant E-cadherins. The BWZ.muKLRG1 cells express a chimeric receptor that has the extracellular and transmembrane regions of KLRG1 and the cytoplasmic region of mouse T cell receptor ζ chain, which can mediate the activating signal to induce interleukin-2 gene expression. This cell line also harbors a β-galactosidase reporter gene under the control of the interleukin-2 promoter. Thus, the E-cadherin binding to the chimera KLRG1 can stimulate the β-galactosidase expression. The W2A, V3A, I4A, and P5A E-cadherin mutants failed to induce β-galactosidase expression (Fig. 3*B*). In contrast, the wild-type and D1A E-cadherins induced the expression of β-galactosidase (Fig. 3*B*). These results are consistent with the SPR and tetramer binding experiments and indicate that the N-terminal region of E-cadherin plays an essential role in KLRG1-mediated cellular signaling.

Killing Assay Using KLRG1-expressing NK Cells—To investigate how much the N-terminal mutations of E-cadherin affect NK cell function, we performed NK cell cytotoxicity assays using the KLRG1-expressing mouse NK cell line, NK03. BW5147 cells expressing wild-type or mutant E-cadherin were used as target cells in the killing assays, which were performed as described under "Experimental Procedures." The expression of wild-type E-cadherin protected target cells from killing by KLRG1-expressing NK03 cells. This protection was reversed in the presence of the $F(ab')_2$ fragment of anti-KLRG1 antibody 3D4, which inhibits the KLRG1-E-cadherin interaction (Fig. 3, *C* and *D*). Target cells expressing wild-type E-cadherin did not show any difference of killing by KLRG1-deficient NK03 cells in the presence or absence of the anti-KLRG1 3D4 $F(ab')_2$ (data not shown). Similar data were obtained using cells expressing the D1A mutant E-cadherin, consistent with the KLRG1-E-cadherin binding and reporter cell assays. On the other hand, target cells expressing the W2A, V3A, and I4A mutant E-cadherins were killed by KLRG1-expressing NK03 cells at similar levels both in the presence and absence of the anti-KLRG1 3D4 $F(ab')_2$. These results show that E-cadherin mutants that abrogate binding also abolish KLRG1-mediated inhibition of killing by KLRG1-expressing NK03 cells (Fig. 3, *C* and *D*). These results indicate that the N-terminal amino acids of E-cadherin are critical for the KLRG1-mediated inhibition of NK cell cytotoxicity.

DISCUSSION

E-cadherin is expressed mainly by epithelial cells and mediates Ca^{2+}-dependent cell-cell adhesion. The N-terminal regions of cadherins are known to play an important role in homotypic adhesion (14, 17). The N-terminal region of E-cadherin can adopt two conformations. In the intramolecular conformation, Trp^2 interacts with Glu^{89} and Met^{92}. In the intermolecular conformation, the N-terminal region can dock with domain 1 of another cadherin to form an adhesive dimer, in which strand exchange occurs (Fig. 4, *left*) (21). This study shows that KLRG1 recognizes a relatively broad area of the N-terminal region of E-cadherin (Trp^2–Pro^6), which largely overlaps with the strand-exchanged homodimer interface. In addition, cells expressing E-cadherin mutants (W2A, V3A, I4A, and P5A) could not interact with KLRG1 tetramer or induce intracellular signaling of KLRG1 reporter cell lines. Further, the expression of the N-terminal mutant E-cadherins (W2A, V3A, I4A) on target cells did not inhibit the cytotoxic activity of KLRG1-expressing NK cells. These results demonstrate that KLRG1 specifically recognizes the strand-exchanged homodimeric interface of E-cadherin, indicating that KLRG1 only binds to the monomeric form of E-cadherin, with an

balt3/zbc-bc/zbc-bc/zbc04409/zbc9087-09z xppws S=1 21/8/09 8:31 4/Color Figure(s) F2,4 ARTNO: M109.038802

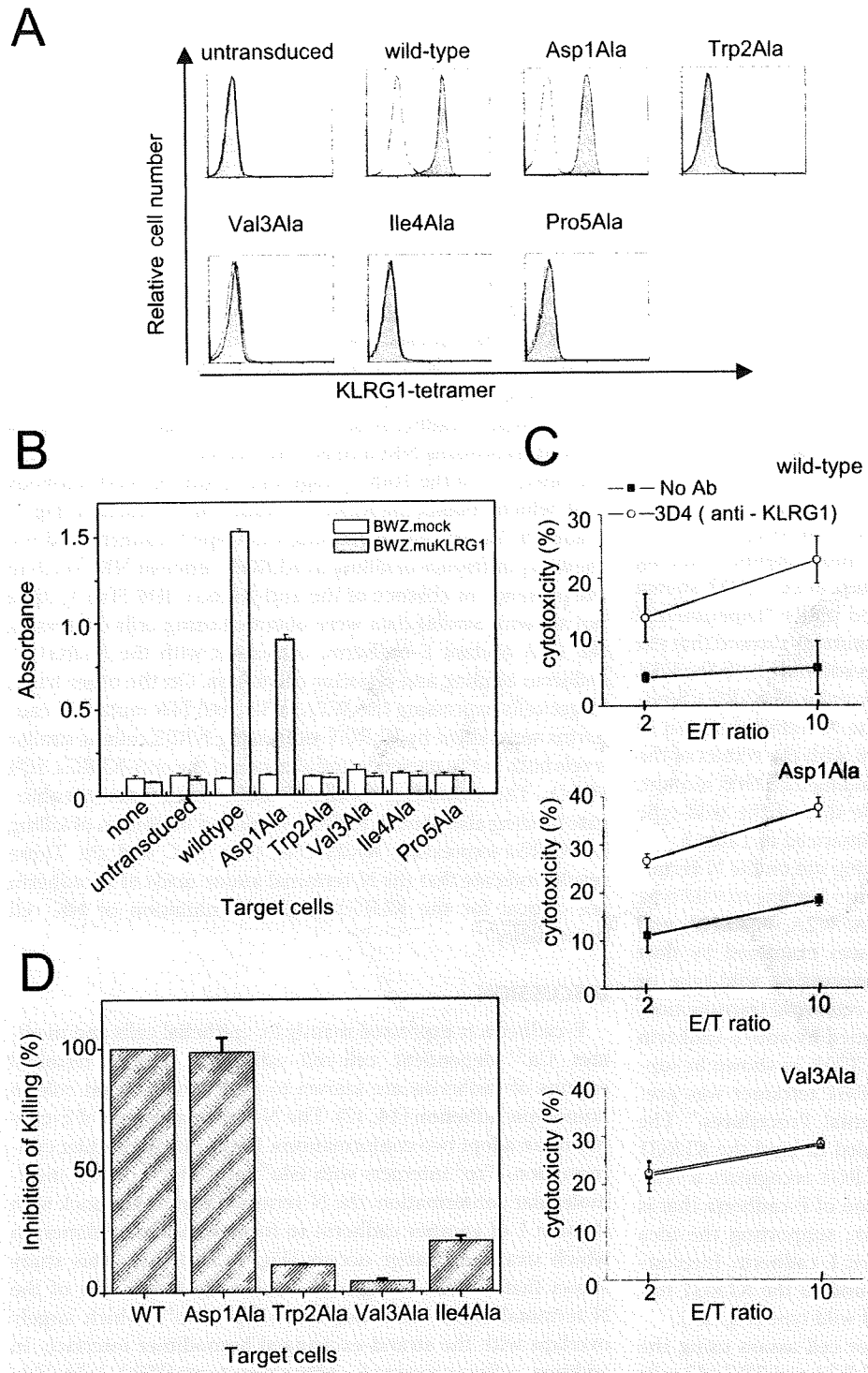

FIGURE 3. **Effects of E-cadherin mutagenesis on KLRG1 tetramer binding, reporter cell assays, and KLRG1-expressing NK cell killing assays.** *A*, untransduced BW5147 cells or BW5147 cells transduced with wild-type or mutant E-cadherin (D1A, W2A, V3A, I4A, and P5A) were stained with KLRG1 tetramer (*shaded histograms*) or PE-streptavidin (*thin lines*). *B*, KLRG1 reporter cells were stimulated with the indicated target cells for 16 h and assayed for β-galactosidase activity. The *bars* represent the relative activities. *C*, KLRG1-expressing NK03 cell killing assays against BW5147 cells expressing wild-type or mutant E-cadherins. The assays were performed in the presence or absence of the anti-KLRG1 3D4 F(ab')$_2$. Representative data for wild-type, D1A, and V3A E-cadherins are shown. *D*, *bar* (mean ± S.D.) indicates the differences of KLRG1-expressing NK03 cell cytotoxicity against target cells expressing the indicated E-cadherins in the presence and absence of the anti-KLRG1 3D4 F(ab')$_2$. The difference of target cells expressing wild-type E-cadherin was set as 100%.

exposed N-terminal region, to regulate immune function, such as NK cell cytotoxicity.

In normal epithelial tissues, two E-cadherin molecules interact with each other to form strand-exchanged homodimeric complexes constituting adherent junctions, as described above, and thus they are not easily accessible to NK cells or T cells (Fig. 4, *left*). However, E-cadherin may be exposed on the surfaces of disrupted or infected epithelial cells. In turn, NK cells and T cells can directly detect E-cadherin by utilizing KLRG1, but this recognition occurs in a more sophisticated manner. Here, we show that KLRG1 recognizes the N-terminal strand-exchanged homodimer interface of E-cadherin and thus can only bind to the monomeric form to inhibit KLRG1-mediated cytotoxicity. This monomeric form is thought to be expressed on abnormal epithelial tissues. Therefore, NK cells and T cells can mediate suitable inhibitory responses via KLRG1 binding to only monomeric E-cadherin. The KLRG1-E-cadherin interaction is presumably safe and efficient for inhibiting the excess functional responses of NK cells as well as those of the SLECs (Fig. 4, *right*). This function is similar to that of inhibitory costimulatory molecules, such as CTLA4 (cytotoxic T-lymphocyte antigen 4).

The $\alpha_E\beta_7$ integrin (CD103) receptor also recognizes E-cadherin (22). The $\alpha_E\beta_7$ integrin is found on intraepithelial lymphocytes, where it mediates their adhesion to epithelial cells and enhances their function (23). The $\alpha_E\beta_7$ integrin recognizes the conserved residue Glu^{31} and its surrounding area at the top of E-cadherin domain 1 (supplemental Fig. S3) (23), adjacent to the KLRG1 binding site. Thus, KLRG1 may physically interfere with $\alpha_E\beta_7$ integrin binding. Although the expression of KLRG1 in activated intraepithelial lymphocytes has not been determined, if KLRG1 is expressed simultaneously with $\alpha_E\beta_7$ integrin, it may inhibit excess immune responses both by trans-

Molecular Basis for KLRG1-E-cadherin Recognition

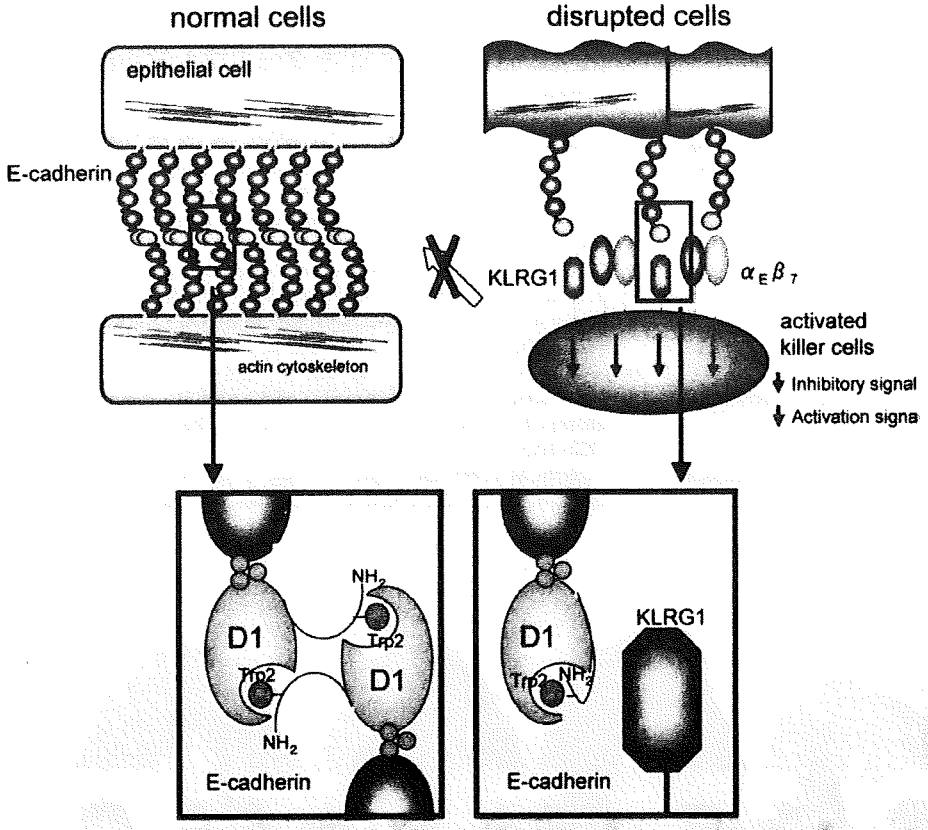

FIGURE 4. **Predicted mechanism of E-cadherin recognition by KLRG1.** *Top*, schematic representation of a normal adherens junction (*left*), comprising the homodimeric interactions of E-cadherins (*colored circles* indicate cadherin domains) and disrupted or infected tissues (*right*), which are recognized by NK or T cells (*large green circle*). *Bottom*, the strand-exchanged homodimeric interactions of EC-D1 (*black line*, N-terminal strand; *orange ball*, Trp2; *orange circle*, EC-D1) are shown at the *bottom left*. KLRG1 (*deep blue angular shapes*), expressed on NK or T cells, recognizes monomeric E-cadherin on disrupted cells. The $\alpha_E\beta_7$ integrin, shown in *pink circles*, may be expressed on KLRG1-expressing lymphocytes to compete with E-cadherin binding and signaling by KLRG1.

ducing E-cadherin-mediated inhibitory signals and by competing for $\alpha_E\beta_7$ integrin binding. Interestingly, $\alpha_E\beta_7$ integrin can bind to both monomeric and homodimeric E-cadherin, whereas KLRG1 binds only monomeric E-cadherin. This functional difference may have a sophisticated potential to finely modulate mucosal immunity (24) as well as NK and T cell development/differentiation.

Several types of cancer cells express mutant E-cadherin. One alteration of the E-cadherin gene is induced by the in-frame skipping of either exon 8 or exon 9. Interestingly, these alterations result in the deletion of either domain 2 or domain 3 of E-cadherin and are reported to abolish KLRG1 binding (25). However, our data suggest that the KLRG1 binding site is located in the N-terminal region, far from domains 2 and 3. Thus, these mutations may indirectly disrupt the conformation of the N-terminal region that is required for KLRG1 recognition. A definitive conclusion will require future investigations of the structural characteristics of the E-cadherin mutants and KLRG1 binding interaction.

The mutation or lack of E-cadherin in some cancer cells causes the loss of cell adhesion and the subsequent acquisition of cellular motility, facilitating tumor metastasis. Such abnormal cells may be susceptible to NK cells and T cells, because of the lack of KLRG1-mediated inhibitory signals. On the other hand, some tumors may exploit the KLRG1-E-cadherin interaction to their advantage. Such tumor cells might initially down-regulate E-cadherin to acquire motility and metastatic potential but then re-express E-cadherin to establish adherent metastatic foci and avoid immune attack by NK cells and T cells (24–27). Therefore, the development of inhibitors of KLRG1-E-cadherin recognition is important for eliminating these cancer cells. Our results demonstrate that KLRG1 recognizes the N-terminal amino acids of monomeric E-cadherin domain 1, which are well conserved in the type I classical cadherins (Fig. 2*D*). In fact, KLRG1 can also bind to the other type I classical cadherins, neuronal and retinal (N- and R-cadherins) (5), strongly suggesting that the N-terminal amino acids are a major determinant for the KLRG1 binding. Therefore, the N-terminal region may be a useful template for designing inhibitors of the KLRG1-E-cadherin interaction.

CONCLUSIONS

This study demonstrates that KLRG1 recognizes the N-terminal region of E-cadherin, known to be critical for homophilic adhesion. Therefore, we propose that KLRG1 cannot bind to the homodimeric form of E-cadherin but rather binds to the monomeric form. The monomeric form of E-cadherin is exposed on the adherens junction in special conditions, such as damaged epithelial tissues. Under these circumstances, it may serve as a target for KLRG1 recognition to mediate inhibitory signals, raising the activation threshold of NK cells and T cells and preventing excessive immune response.

Acknowledgments—We thank T. Saito, Y. Ishino, D. Kohda, T. Sugi, and K. Morikawa for helpful discussions. We thank S. Grzesick for providing the NMR assignment data for E-cadherin. We thank T. Matsukura for providing anti-KLRG1 monoclonal antibody.

REFERENCES

1. Biron, C. A., Nguyen, K. B., Pien, G. C., Cousens, L. P., and Salazar-Mather, T. P. (1999) *Annu. Rev. Immunol.* **17**, 189–220
2. Lanier, L. L. (2005) *Annu. Rev. Immunol.* **23**, 225–274
3. Moretta, L., and Moretta, A. (2004) *Curr. Opin. Immunol.* **16**, 626–633
4. Yokoyama, W. M. (1998) *Curr. Opin. Immunol.* **10**, 298–305
5. Ito, M., Maruyama, T., Saito, N., Koganei, S., Yamamoto, K., and Matsumoto, N. (2006) *J. Exp. Med.* **203**, 289–295
6. Gründemann, C., Bauer, M., Schweier, O., von Oppen, N., Lässing, U., Saudan, P., Becker, K. F., Karp, K., Hanke, T., Bachmann, M. F., and

balt3/zbc-bc/zbc-bc/zbc04409/zbc9087-09z xppws S=1 21/8/09 8:31 4/Color Figure(s) F2,4 ARTNO: M109.038802

Pircher, H. (2006) *J. Immunol.* **176,** 1311–1315
7. Robbins, S. H., Tessmer, M. S., Mikayama, T., and Brossay, L. (2004) *J. Immunol.* **173,** 259–266
8. Robbins, S. H., Nguyen, K. B., Takahashi, N., Mikayama, T., Biron, C. A., and Brossay, L. (2002) *J. Immunol.* **168,** 2585–2589
9. Huntington, N. D., Tabarias, H., Fairfax, K., Brady, J., Hayakawa, Y., Degli-Esposti, M. A., Smyth, M. J., Tarlinton, D. M., and Nutt, S. L. (2007) *J. Immunol.* **178,** 4764–4770
10. Joshi, N. S., Cui, W., Chandele, A., Lee, H. K., Urso, D. R., Hagman, J., Gapin, L., and Kaech, S. M. (2007) *Immunity* **27,** 281–295
11. Gooding, J. M., Yap, K. L., and Ikura, M. (2004) *BioEssays* **26,** 497–511
12. Takeichi, M. (1991) *Science* **251,** 1451–1455
13. Gumbiner, B. M. (2000) *J. Cell Biol.* **148,** 399–404
14. Pokutta, S., and Weis, W. I. (2007) *Annu. Rev. Cell Dev. Biol.* **23,** 237–261
15. Overduin, M., Harvey, T. S., Bagby, S., Tong, K. I., Yau, P., Takeichi, M., and Ikura, M. (1995) *Science* **267,** 386–389
16. Shapiro, L., Fannon, A. M., Kwong, P. D., Thompson, A., Lehmann, M. S., Grübel, G., Legrand, J. F., Als-Nielsen, J., Colman, D. R., and Hendrickson, W. A. (1995) *Nature* **374,** 327–337
17. Nose, A., Tsuji, K., and Takeichi, M. (1990) *Cell* **61,** 147–155
18. Rosshart, S., Hofmann, M., Schweier, O., Pfaff, A. K., Yoshimoto, K., Takeuchi, T., Molnar, E., Schamel, W. W., and Pircher, H. (2008) *Eur. J. Immunol.* **38,** 3354–3364
19. Ohki, I., Shimotake, N., Fujita, N., Nakao, M., and Shirakawa, M. (1999) *EMBO J.* **18,** 6653–6661
20. Matsumoto, N., Mitsuki, M., Tajima, K., Yokoyama, W. M., and Yamamoto, K. (2001) *J. Exp. Med.* **193,** 147–158
21. Parisini, E., Higgins, J. M., Liu, J. H., Brenner, M. B., and Wang, J. H. (2007) *J. Mol. Biol.* **373,** 401–411
22. Cepek, K. L., Shaw, S. K., Parker, C. M., Russell, G. J., Morrow, J. S., Rimm, D. L., and Brenner, M. B. (1994) *Nature* **372,** 190–193
23. Agace, W. W., Higgins, J. M., Sadasivan, B., Brenner, M. B., and Parker, C. M. (2000) *Curr. Opin. Cell Biol.* **12,** 563–568
24. Colonna, M. (2006) *J. Exp. Med.* **203,** 261–264
25. Schwartzkopff, S., Gründemann, C., Schweier, O., Rosshart, S., Karjalainen, K. E., Becker, K. F., and Pircher, H. (2007) *J. Immunol.* **179,** 1022–1029
26. Takeichi, M. (1993) *Curr. Opin. Cell Biol.* **5,** 806–811
27. Cavallaro, U., and Christofori, G. (2004) *Nat. Rev. Cancer* **4,** 118–132

Biochemical and Biophysical Research Communications xxx (2009) xxx–xxx

Contents lists available at ScienceDirect

Biochemical and Biophysical Research Communications

journal homepage: www.elsevier.com/locate/ybbrc

Silkworm expression and sugar profiling of human immune cell surface receptor, KIR2DL1

Kaori Sasaki [a], Mizuho Kajikawa [a], Kimiko Kuroki [a], Tomoko Motohashi [b], Tsukasa Shimojima [b], Enoch Y. Park [c], Sachiko Kondo [d,e], Hirokazu Yagi [e], Koichi Kato [d,e,f,g], Katsumi Maenaka [a,*]

[a] Medical Institute of Bioregulation, Kyushu University, 3-1-1 Maidashi, Higashi-ku, Fukuoka 812-8582, Japan
[b] National Institute of Genetics, 1111 Yata, Mishima 411-8540, Japan
[c] Laboratory of Biotechnology, Department of Applied Biological Chemistry, Shizuoka University, 836 Ohya, Suruga-ku, Shizuoka, Shizuoka 422-8529, Japan
[d] GLYENCE, 2-22-8 Chikusa, Chikusa-ku, Nagoya 464-0858, Japan
[e] Graduate School of Pharmaceutical Sciences, Nagoya City University, 3-1 Tanabe-dori, Mizuho-ku, Nagoya 467-8603, Japan
[f] Institute for Molecular Science and Okazaki Institute for Integrative Bioscience, National Institutes of National Science, 5-1 Higashiyama Myodaiji, Okazaki 487-8501, Japan
[g] The Glycoscience Institute, Ochanomizu University, 2-1-1 Ohtsuka, Bunkyo-ku, Tokyo 112-8610, Japan

ARTICLE INFO

Article history:
Received 2 July 2009
Available online xxxx

Keywords:
Bacmid
BmNPV
Bombyx mori
Silkworm
Baculovirus expression system
Killer cell Ig-like receptor
N-glycosylation

ABSTRACT

Immune cell surface receptors are directly involved in human diseases, and thus represent major drug targets. However, it is generally difficult to obtain sufficient amounts of these receptors for biochemical and structural studies because they often require posttranslational modifications, especially sugar modification. Recently, we have established a bacmid expression system for the baculovirus BmNPV, which directly infects silkworms, an attractive host for the large-scale production of recombinant sugar-modified proteins. Here we produced the human immune cell surface receptor, killer cell Ig-like receptor 2DL1 (KIR2DL1), by using the BmNPV bacmid expression system, in silkworms. By the direct injection of the bacmid DNA, the recombinant KIR2DL1 protein was efficiently expressed, secreted into body fluids, and purified by Ni^{2+} affinity column chromatography. We further optimized the expression conditions, and the final yield was 0.2 mg/larva. The sugar profiling revealed that the *N*-linked sugars of the purified protein comprised very few components, two paucimannose-type oligosaccharides, Manα1-6Manβ1-4GlcNAcβ1-4GlcNAc and Manα1-6Manβ1-4GlcNAcβ1-4(Fucα1-6)GlcNAc. This revealed that the protein product was much more homogeneous than the complex-sugar type product obtained by mammalian cell expression. The surface plasmon resonance analysis demonstrated that the purified KIR2DL1 protein exhibited specific binding to the HLA-Cw4 ligand. Moreover, the CD spectrum showed the proper secondary structure. These results clearly suggested that the silkworm expression system is quite useful for the expression of cell surface receptors that require posttranslational modifications, as well as for their structural and binding studies, due to the relatively homogeneous *N*-linked sugar modifications.

Introduction

The cell surface receptors of immune cells regulate various biological functions via highly specific binding to their cognate ligands. Immune cell surface receptors tend to be directly involved in immune-related diseases, and thus they are one of the main targets for drug design. Moreover, the soluble forms of such receptors and their specific antibodies could become biopharmaceutical drugs for immune regulation. However, it is presently difficult to obtain sufficient amounts of the immune cell surface receptors for biochemical and structural studies, because they generally require sugar modifications. The baculovirus expression vector system (BEVS) is quite useful for the preparation of such post-translationally-modified recombinant proteins.

There are two types of baculoviruses currently utilized in BEVS. One of them is *Autographa californica* nuclear polyhedrosis virus (AcNPV), which can infect only *Spodoptera frugiperda* and *Tricoplusia ni*. The AcNPV BEVS is widely used and commercially available. The other is the *Bombyx mori* nuclear polyhedrosis virus (BmNPV), which can only infect the silkworm and its cell lines. The BmNPV BEVS using silkworms is one of the most suitable systems, because silkworms, which produce extreme amounts of silk fibers containing fibroin, are very attractive as a protein-production factory. Indeed, the protein expression using silkworms is 10- to 100-fold higher than that using *B. mori* cells. The conventional BmNPV BEVS, which requires a difficult, time-consuming plaque assay technique to obtain the recombinant viruses, was successfully utilized for the expression of interleukin receptors and interferon-α [1,2].

* Corresponding author. Fax: +81 92 642 6998.
E-mail address: kmaenaka-umin@umin.net (K. Maenaka).

0006-291X/$ - see front matter © 2009 Elsevier Inc. All rights reserved.
doi:10.1016/j.bbrc.2009.07.065

Please cite this article in press as: K. Sasaki et al., Silkworm expression and sugar profiling of human immune cell surface receptor, KIR2DL1, Biochem. Biophys. Res. Commun. (2009), doi:10.1016/j.bbrc.2009.07.065

The AcNPV BEVS employs a very useful bacmid DNA comprising the baculoviral DNA genome with the *Escherichia coli* origin and transposition sequences. Since the replication of bacmid DNA and the transposition of the desired genes of the transfer vector onto the bacmid DNA can occur in *E. coli*, the time-consuming preparation of recombinant viruses, as described above, is not required. The BmNPV bacmid DNA, which we recently developed [3], can be mixed with a lipid reagent and directly injected into the silkworm for the infection. Therefore, this bacmid system for silkworms is quite useful and was long-awaited. Recently, using the BmNPV bacmid-silkworm expression system, we successfully produced a human G-protein coupled receptor (GPCR), nociceptin receptor, in the membranes of fat bodies as well as on the viral surface [4].

Human killer cell Ig-like receptor 2DL1 (KIR2DL1) is an immune cell surface receptor that is mainly expressed on natural killer (NK) cells and some subsets of T cells [5–7]. KIR2DL1 recognizes the human major histocompatibility complex (MHC) class I molecule, HLA-Cw4 (and its relatives) on target cells, and has inhibitory motifs (immunoreceptor tyrosine-based inhibitory motifs) to suppress the immune responses of NK cells and T cells upon binding to HLA-Cw4 [8–10]. Viral infection and tumorigenesis often reduce the expression of MHCI to evade the T cell responses, in which T cell receptors specifically recognize the unusual peptide displayed by MHCIs for the activation. These cells exhibiting reduced or no MHCI expression can potentially become susceptible to KIR-expressing immune cells, because they lack KIR-mediated inhibitory signals. Genetic analyses clearly demonstrated that the KIR genes are associated with infectious diseases, autoimmune diseases, and cancer [11,12]. The accumulated evidence has revealed the physiological significance of KIR2DL1 in immune regulation.

We now report the successful high-level expression of the extracellular region of KIR2DL1, as a secreted protein in the body fluid of silkworm larvae, using the BmNPV BEVS. We also established a purification method for the secreted protein from the body fluid, using His6-tag affinity chromatography. Furthermore, we analyzed the sugar content of the purified protein, which revealed that the protein harbored two kinds of paucimannose-type oligosaccharides, Manα1-6Manβ1-4GlcNAcβ1-4(Fucα1-6)GlcNAc and Manα1-6Manβ1-4GlcNAcβ1-4GlcNAc. On the other hand, a previous report found that the IgG antibody expressed in silkworms using our BmNPV BEVS exclusively possessed two kinds of paucimannose-type oligosaccharides, Manα1-6Manβ1-4GlcNAcβ1-4(Fucα1-6)GlcNAc and Manα1-6(Manα1-3)Manβ1-4GlcNAcβ1-4(Fucα1-6)GlcNAc [13]. The major species was the same, but the minor one was different. Structural and functional studies of the purified KIR2DL1 protein were performed. The surface plasmon resonance analysis revealed that the protein bound to its HLA-Cw4 ligand, and the CD spectrum indicated the correct folding. Therefore, the BmNPV bacmid-silkworm expression system

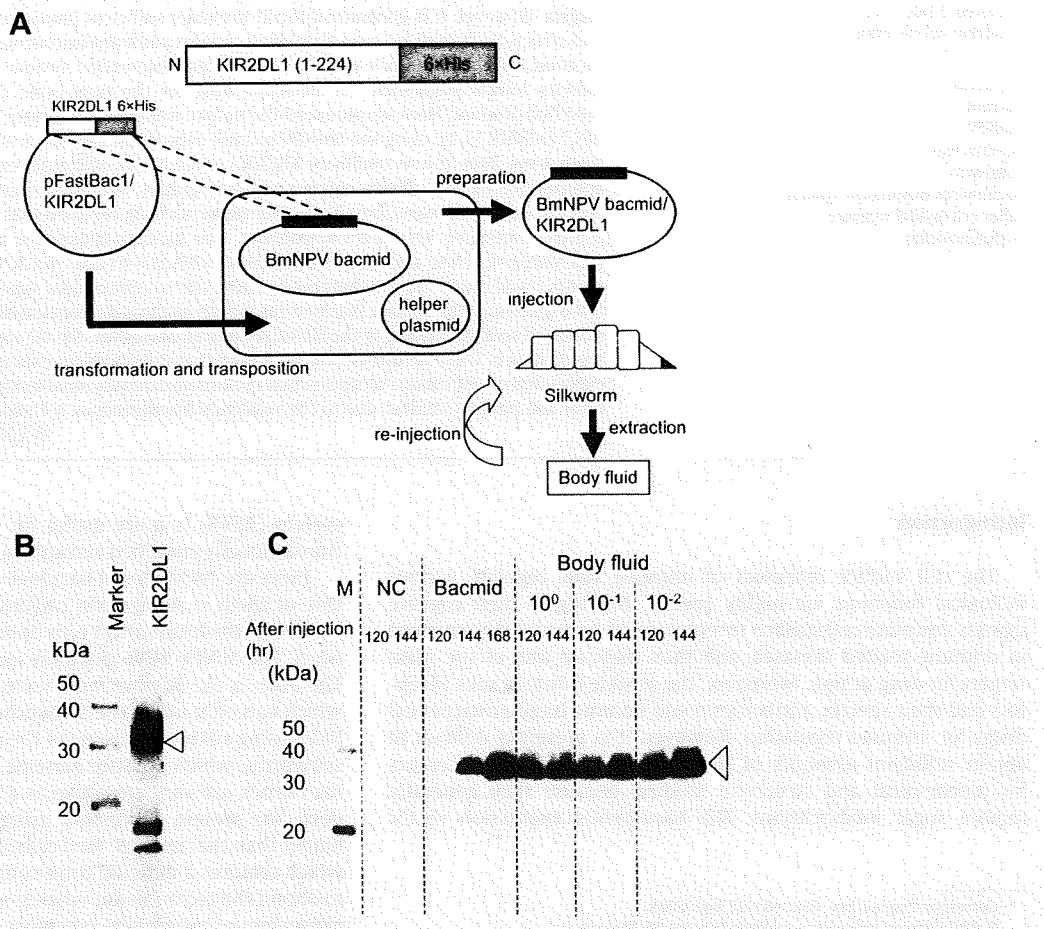

Fig. 1. (A) Construction of the recombinant BmNPV bacmid DNA and expression strategy using silkworm larvae. (B) Western blot analysis for detection of the expressed KIR2DL1 protein in the hemolymph of silkworms, using an anti-pentahistidine antibody. (C) Western blot analysis for the detection of the recombinant KIR2DL1 protein (open arrowhead) expressed by the injection of BmNPV bacmid DNA or body fluid solution. NC, negative control.

Please cite this article in press as: K. Sasaki et al., Silkworm expression and sugar profiling of human immune cell surface receptor, KIR2DL1, Biochem. Biophys. Res. Commun. (2009), doi:10.1016/j.bbrc.2009.07.065

combined with the affinity-tag purification technique is quite useful for the rapid and efficient production of cell surface antigens/receptors, as secreted, soluble proteins.

Materials and methods

Construction of the BmNPV bacmid expressing KIR2DL1. The gene encoding the extracellular region of KIR2DL1 was obtained by PCR, using the following primers (forward, 5′-TTAGGATCCATGTCGC TCTTGGTCGTCAGC-3′; reverse, 5′-TTAGAATTCTTAATGATGATGAT GATGATGGTGCAGGTGTCGGGGGTTACC-3′) from pKMATHNK1 [10]. The sequence encoding the hexahistidine tag was introduced at the 5′ end of the reverse primer for further purification. The KIR2DL1 gene was inserted into the donor plasmid pFastBac1 vector. The resultant plasmid was designated as pFastBac1/KIR2DL1. Transposition was carried out by transforming the plasmid pFastBac1/KIR2DL1 into BmDH10Bac cells [3]. White kanamycin- and gentamycin-resistant colonies were selected, and then the BmNPV bacmid, designated as BmNPV bacmid/KIR2DL1, was isolated.

Expression of the KIR2DL1 gene in silkworm larvae and protein purification. We used the first day of fifth instar larvae for the injection or infection. Silkworm larvae were directly injected with the BmNPV bacmid/KIR2DL1. The BmNPV bacmid/KIR2DL1 (1.0 μg) was suspended in 3 μl of DMRIE-C reagent and the resultant mixture was injected into the dorsal side of the larvae.

After the larvae were cultured for 144 h, the hemolymph was collected and immediately combined with sodium thiosulfate. The collected hemolymph was diluted in buffer A (20 mM Tris–HCl (pH 8.0), 100 mM NaCl). The recombinant proteins were purified by using Ni Sepharose 6 Fast Flow resin (GE Healthcare).

SDS–PAGE and Western blotting analysis. In order to perform sodium dodecyl sulfate–polyacrylamide gel electrophoresis (SDS–PAGE), the eluted fractions were loaded on a 15–25% slab gel, and then stained with Coomassie brilliant blue. For Western blotting, the proteins, separated by SDS–PAGE as described above, were transferred onto a polyvinylidene difluoride (PVDF) membrane. The membrane was incubated in PBS-T containing a 1/1000 dilution of the penta-His antibody (Qiagen) and then incubated with a horseradish peroxidase labeled mouse IgG antibody (Amersham Biosciences, Piscataway, NJ). After washing with PBS-T, the detection was carried out using an ECL Plus Western Blotting Detection System (GE Healthcare).

Surface plasmon resonance (SPR) and circular dichroism spectroscopy (CD). SPR measurements were performed using a BIAcore 2000 instrument (GE Healthcare). As described in our previous report [10], the HLA-Cw4 was immobilized, and the binding assay was performed, using serial dilutions of the KIR2DL1 ranging from 0.06 to 30 μM. The CD spectra of a 7.2 μM solution of KIR2DL1 were measured with a Jasco-J 720 spectropolarimeter.

Sugar digestion and profiling analysis. The KIR2DL1 protein was digested with either EndoH (New England Biolabs, MA, USA) or PNGaseF (New England Biolabs) and then subjected to SDS–PAGE to determine the existence of *N*-glycan and its EndoH sensitive sugars. Furthermore, a detailed sugar composition analysis was performed by the method described in our previous reports [14–16]. Briefly, the KIR2DL1 protein (0.3 mg) was proteolyzed with chymotrypsin and trypsin mixture, and was further digested with glycoamidase A to release *N*-glycans. After the removal of the peptide materials, the reducing ends of the resultant *N*-glycans (PA-oligosaccharides) were derivatized with 2-aminopyridine (Wako, Osaka, Japan). The PA-glycan mixture was separated by an octadecyl silica (ODS) column (Shimadzu, Kyoto), and the recorded elution time represents the glucose unit (GU) value. The individual fractions were subjected to matrix-assisted laser desorption/ionization-time of flight mass spectrometry (MALDI-TOF-MS). The identification of *N*-glycan structures was based on GU and mass values in comparison to PA-glycans in the GALAXY database (http://www.glycoanalysis.info/galaxy2/ENG/systemin1.jsp) [17]. The *N*-glycans were confirmed by co-chromatography on the ODS column.

Results

Expression of KIR2DL1 in silkworms by direct injection of its bacmid DNA

First, we constructed the BmNPV bacmid/KIR2DL1, bearing the gene encoding the extracellular region (residues 1–224) of the human immune cell surface receptor, killer cell immunoglobulin-like receptor (KIR) 2DL1, under the control of the polyhedrin promoter and with a hexahistidine tag at the C-terminus (summarized in Fig. 1A). The obtained bacmid DNA (0.3 μg) was directly injected into the fifth instar silkworm body. Six days after the injection, the body hemolymph was collected and centrifuged at 10,000*g* for 10 min, and 0.5 μl of the hemolymph was used for Western blotting. The Western blotting analysis using the anti-pentahistidine

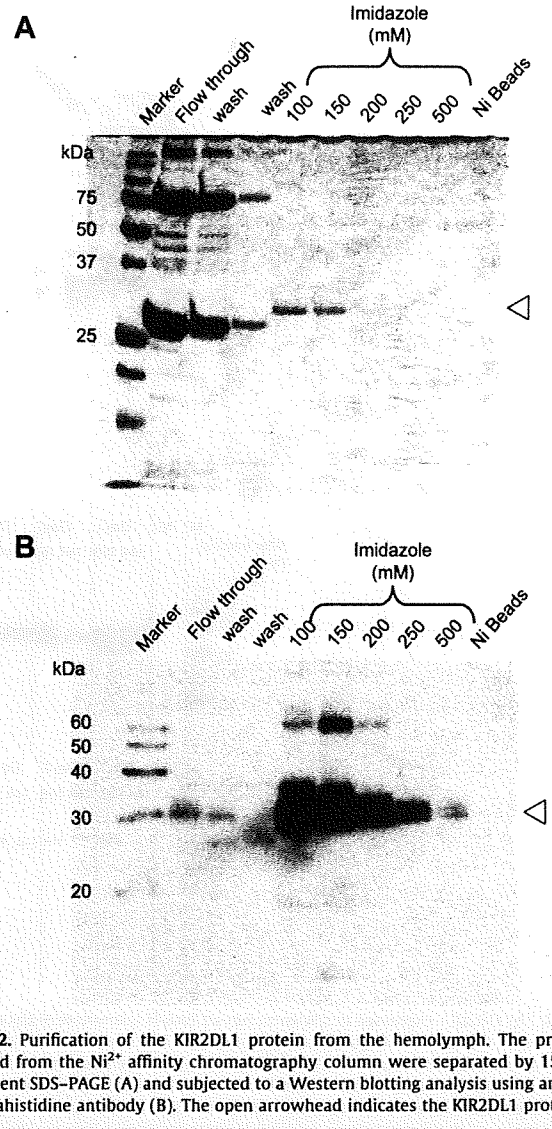

Fig. 2. Purification of the KIR2DL1 protein from the hemolymph. The proteins eluted from the Ni^{2+} affinity chromatography column were separated by 15–25% gradient SDS–PAGE (A) and subjected to a Western blotting analysis using an anti-pentahistidine antibody (B). The open arrowhead indicates the KIR2DL1 protein.

antibody clearly showed that the recombinant KIR2DL1 protein was expressed in the hemolymph of silkworm by the direct bacmid DNA injection method (Fig. 1B). To optimize the expression conditions of this system, different amounts of injected bacmid DNA were examined, and the largest expression of the recombinant protein was obtained by injecting 1.0 μg of DNA.

Furthermore, the body fluid derived from the silkworm larvae expressing the recombinant KIR2DL1 protein included a large amount of recombinant baculovirus. Thus, in terms of experimental cost and time to produce the protein, it is worth examining the effectiveness of directly injecting the body fluid into other larvae. The needles, which were briefly dipped into the body fluid solutions at several diluted concentrations, were used to penetrate the silkworm larvae, and the expression levels were evaluated by Western blotting using an anti-pentahistidine antibody. As clearly shown in Fig. 1C, even 100-times-diluted body fluid still exhibited sufficient infectivity (also confirmed by Western blotting using an anti-gp64 (BmNPV envelope protein) antibody) and conferred the stable expression of a large amount of the KIR2DL1 protein. Therefore, the injection of the body fluid including the recombinant viruses remarkably reduces both the cost and time, as compared with that of the bacmid DNA, which requires the DNA preparation and the lipid reagent for the infection.

Purification from hemolymph

The hemolymph including the recombinant KIR2DL1 protein was collected by using a needle to puncture the abdominal leg of silkworm larvae, and sodium thiosulfate was immediately added to prevent melanization. The hemolymph solution was subjected to Ni^{2+} affinity column chromatography for the purification. The SDS–PAGE displayed a single band of about 30 kDa of the KIR2DL1 protein in the fractions eluted with 100 or 150 mM imidazole, and the protein was further confirmed by Western blotting using an anti-pentahistidine antibody (Fig. 2). For biochemical characterizations, the protein was further purified by anion-exchange chromatography. The final yield was 0.2 mg of the purified protein from one larva. Several larvae can easily produce mg quantities of the recombinant protein, and thus this system can achieve high-level expression at a low cost and a short time period.

Characterization of the recombinant KIR2DL1 expressed in silkworms

For the molecular characterization of the KIR2DL1 protein expressed in the hemolymph of silkworm, several biochemical analyses were performed. To determine whether the recombinant protein was *N*-glycosylated, it was treated with EndoH or PNGase F,

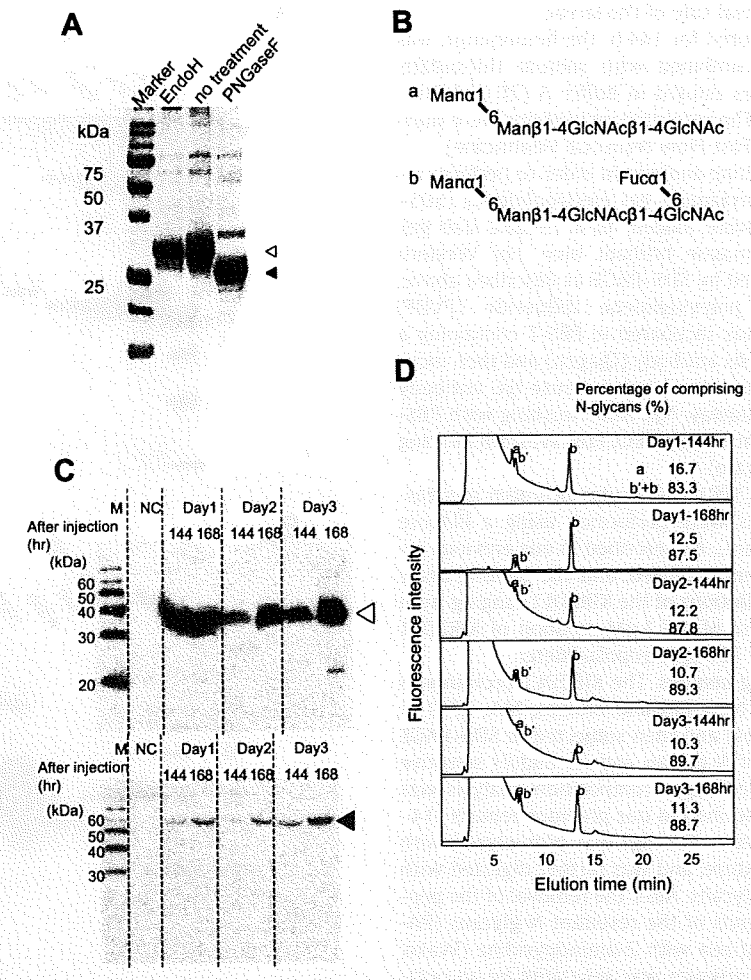

Fig. 3. (A) KIR2DL1 expressed in silkworm has an EndoH insensitive *N*-glycan modification. The open arrowhead indicates the glycosylated KIR2DL1 protein, and the filled arrowhead indicates the deglycosylated protein. (B) The structures of the PA-oligosaccharides obtained from the KIR2DL1 protein expressed in silkworm hemolymph. Western blot analysis (C) and *N*-linked sugar profile (D) of the recombinant KIR2DL1 expressed at different injection and extraction times. Day 1 indicates the first day of fifth instars. (C) The open arrowhead indicates the KIR2DL1 protein, and the filled arrowhead indicates gp64. (D) The structures of *N*-linked sugars were determined by HPLC and MS, as described under Materials and methods. In (D), b′ indicates epimerized b, which is a byproduct obtained during the 2-aminopyridine derivatization reaction.

Please cite this article in press as: K. Sasaki et al., Silkworm expression and sugar profiling of human immune cell surface receptor, KIR2DL1, Biochem. Biophys. Res. Commun. (2009), doi:10.1016/j.bbrc.2009.07.065

which eliminate the *N*-linked sugars differently (PNGase F cleaves any kind of *N*-linked sugar except for α-1,3-fucose-containing glycans, while EndoH digests the high mannose and some hybrid oligosaccharides of *N*-linked sugars). The PNGase F treatment shifted the band of the KIR2DL1 protein to a lower position in the SDS–PAGE gel, but the EndoH treatment did not (Fig. 3A). This result indicated that the obtained protein was *N*-glycosylated, but its *N*-linked sugars were not EndoH-sensitive. A further sugar composition analysis was performed, using a combination of HPLC and MS. It revealed that the appended sugar of the protein consisted of only two kinds of small paucimannose-type sugars, Manα1-6Manβ1-4GlcNAcβ1-4(Fucα1-6)GlcNAc and Manα1-6Manβ1-4GlcNAcβ1-4GlcNAc (Fig. 3B). The former one was significantly predominant (83–90%) over the latter (10–17%). Interestingly, the sugar composition of the paucimannose-type oligosaccharides was maintained under the different expression conditions, in terms of the injection times and expression levels (Fig. 3C–D). Although the sugar content was slightly different from that of the previously reported IgG antibody [13], the relatively homogeneous and small sugar modifications seem potentially useful for structural studies.

Next, we analyzed the binding ability of the recombinant KIR2DL1 protein to its ligand, HLA-Cw4, by surface plasmon resonance (SPR). As shown in Fig. 4, the purified KIR2DL1 specifically recognized HLA-Cw4, with a K_d of 8.6 ± 0.69 μM, although no binding to HLA-A11 and BSA was observed. Furthermore, the CD spectrum of the KIR2DL1 protein displayed the typical β-sheet secondary structure (data not shown), which corresponds to the β-sandwich feature in the crystal structure of KIR2DL1 [18]. Taken together, these results clearly indicated that the silkworm could produce the KIR2DL1 protein with the proper structural and functional features.

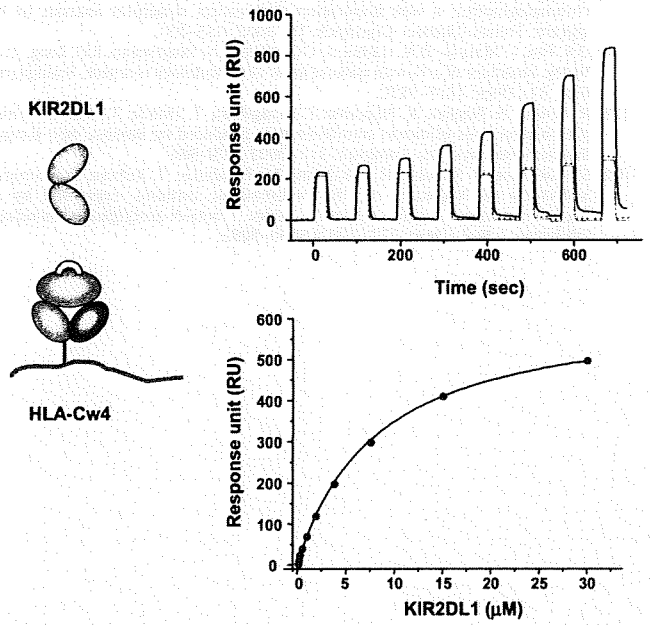

Fig. 4. SPR binding analysis. Left: Schematic representation of the binding study between the soluble KIR2DL1 protein (cyan) expressed in silkworm and the immobilized HLA-Cw4 (orange and purple). Right: Equilibrium binding of KIR2DL1 to immobilized HLA-Cw4. The KIR2DL1 solution was injected for 30 s through flow cell 1 with control (BSA, dotted line), flow cell 2 with HLA-A11 (gray line) and flow cell 3 with HLA-Cw4 (solid line). Plots of the equilibrium binding responses of KIR2DL1 versus concentration. The solid line represents direct nonlinear fits of the 1:1 Langmuir binding isoform to the data. RU, response units. (For interpretation of the references to color in this figure legend, the reader is referred to the web version of this paper.)

Discussion

Immune cell surface receptors are highly glycosylated, and thus it is often difficult to express sufficient amounts of the recombinant proteins. Therefore, an expression system that is easy-to-use and produces a high expression level of post-translationally-modified receptors has been eagerly awaited. Here, we report the successful expression of human killer cell Ig-like receptor 2DL1 by a simple and rapid method combining silkworm expression with the direct injection of the BmNPV bacmid DNA.

The silkworm is a very attractive host for protein production, for the following reasons: (1) simple feeding and low cost: large-scale and time-consuming cell cultivation is not necessary, (2) only a few pieces of indispensable equipment are needed: essentially one incubator for breeding silkworms, (3) high-level protein expression: the very strong polyhedrin promoter and the high expression state are ready for producing silk proteins (fibroins), and (4) the intramolecular disulfide bond formation and the post-translational modifications are similar to those in mammals. Indeed, the present study demonstrated that only a few silkworm larvae (costing only ~20 US dollars) are sufficient to produce ~mg order of immune cell surface receptors.

On the other hand, the BmNPV baculovirus bacmid system [3] also has some remarkable advantages: (1) it is directly applicable to silkworm expression: the commercially available *A. californica* nucleopolyhedrovirus (AcNPV) BEVS normally requires the large-scale cultivation of insect cell lines, (2) it is an easy and quick method: it requires only bacmid DNA, which can replicate in *E. coli* and thus the site-specific transposition for introducing the target gene into bacmid DNA can be done in *E. coli*, while in contrast, a high-titer recombinant virus together with proficient and time-consuming virus-handling techniques are necessary for AcNPV BEVS, (3) high biohazard safety: the bacmid DNA itself lacks infective activity (only gene transfer ability) and the baculoviruses are not infectious to mammalian cells.

Here, using the above-mentioned BmNPV bacmid-silkworm expression system [3], the recombinant KIR2DL1 protein was produced in body fluid only 5–7 days after the injection of DNA into silkworms. The obtained body fluid was applied to a Ni^{2+} affinity column for purification, and 0.2 mg of the highly purified protein could be obtained from one larva. Furthermore, the recombinant baculoviruses, which are easily purified from the body fluid by simple ultracentrifugation steps, could be directly injected into other larvae to stably produce the KIR2DL1 protein (Fig. 1C). This technique is quite useful for the significant reduction of both cost and time. Finally, the standard method for silkworm expression and purification of recombinant cell surface receptors was established.

The sugar modifications are often important for functional and structural analyses, as well as for practical applications. The previous report of the silkworm expression of mouse interferon-β demonstrated that the expressed protein harbored variable sets of paucimannose-type *N*-linked sugars, including Manα1-6Manβ1-4GlcNAcβ1-4GlcNAc (6.4%) and Manα1-6(Manα1-3)Manβ1-4GlcNAcβ1-4(Fucα1-6)GlcNAc (1.1%) [19]. These paucimannose-type sugars are possibly derived from GlcNAcMan5GlcNAc2 by the mannosidase-mediated excision of α-linked mannosyl residues, followed by the GlcNAcase-mediated deletion of a β-1,2-linked terminal GlcNAc residue [20]. In contrast, in the BmNPV bacmid-silkworm expression system, the *N*-linked sugar composition of the expressed KIR2DL1 protein solely comprised two kinds of small paucimannose-type oligosaccharides, Manα1-6Manβ1-4GlcNAcβ1-4(Fucα1-6)GlcNAc (83–90%) and Manα1-6Manβ1-4GlcNAcβ1-4GlcNAc (10–17%). Similarly, the previous report of IgG expressed by the same system revealed that the IgG protein harbored two sugar

Please cite this article in press as: K. Sasaki et al., Silkworm expression and sugar profiling of human immune cell surface receptor, KIR2DL1, Biochem. Biophys. Res. Commun. (2009), doi:10.1016/j.bbrc.2009.07.065

types, Manα1-6Manβ1-4GlcNAcβ1-4(Fucα1-6)GlcNAc (77.5%) and Manα1-6(Manα1-3)Manβ1-4GlcNAcβ1-4(Fucα1-6)GlcNAc (12.7%) [13]. The major one, Manα1-6Manβ1-4GlcNAcβ1-4(Fucα1-6)GlcNAc, was maintained in the expression of different proteins, and thus basically small *N*-linked paucimannose-type sugars were preferable, even though some composition differences were observed. Furthermore, the BmNPV bacmid-silkworm expression did not show any detectable differences in the sugar modifications under various conditions (Fig. 3D). These small and relatively homogeneous *N*-linked sugar modifications in the BmNPV bacmid-silkworm expression system have the potential to be applicable to structural and biochemical studies of immune cell surface receptors.

Taken together, this large-scale and rapid BmNPV bacmid-silkworm production system will be quite useful for future high throughput drug screening as well as for functional and structural studies of human immune cell surface receptors.

Acknowledgments

We thank M. Ohtsu and D. Kohda, Medical Institute of Bioregulation, Kyushu University. K.M. was supported in part by the Ministry of Education, Culture, Sports, Science and Technology and the Ministry of Health, and the Japan Bio-oriented Technology Research Advancement Institute (BRAIN). K. Kato was supported in part by Grant-in-Aid for Scientific Research (B) (21370050) by the Ministry of Education, Culture, Sports, Science and Technology. K. S. and K. Kuroki were supported by research fellowships and a research grant of the Japan Society for the Promotion of Science for young scientists.

References

[1] E. Honjo, Y. Shoyama, T. Tamada, H. Shigematsu, T. Hatanaka, S. Kanaji, K. Arima, Y. Ito, K. Izuhara, R. Kuroki, Expression of the extracellular region of the human interleukin-4 receptor alpha chain and interleukin-13 receptor alpha1 chain by a silkworm-baculovirus system, Protein Expr. Purif. 60 (2008) 25–30.

[2] Z. Na, Y. Huipeng, L. Lipan, C. Cuiping, M.L. Umashankar, L. Xingmeng, W. Xiaofeng, W. Bing, C. Weizheng, J.L. Cenis, Efficient production of canine interferon-alpha in silkworm *Bombyx mori* by use of a BmNPV/Bac-to-Bac expression system, Appl. Microbiol. Biotechnol. 78 (2008) 221–226.

[3] T. Motohashi, T. Shimojima, T. Fukagawa, K. Maenaka, E.Y. Park, Efficient large-scale protein production of larvae and pupae of silkworm by *Bombyx mori* nuclear polyhedrosis virus bacmid system, Biochem. Biophys. Res. Commun. 326 (2005) 564–569.

[4] M. Kajikawa, K. Sasaki, Y. Wakimoto, M. Toyooka, T. Motohashi, T. Shimojima, S. Takeda, E.Y. Park, K. Maenaka, Efficient silkworm expression of human GPCR (nociceptin receptor) by a *Bombyx mori* bacmid DNA system, Biochem. Biophys. Res. Commun. 385 (2009) 375–379.

[5] M. Colonna, Natural killer cell receptors specific for MHC class I molecules, Curr. Opin. Immunol. 8 (1996) 101–107.

[6] E.O. Long, S. Rajagopalan, HLA class I recognition by killer cell Ig-like receptors, Semin. Immunol. 12 (2000) 101–108.

[7] L. Moretta, M.C. Mingari, D. Pende, C. Bottino, R. Biassoni, A. Moretta, The molecular basis of natural killer (NK) cell recognition and function, J. Clin. Immunol. 16 (1996) 243–253.

[8] M. Colonna, J. Samaridis, Cloning of immunoglobulin-superfamily members associated with HLA-C and HLA-B recognition by human natural killer cells, Science 268 (1995) 405–408.

[9] N. Wagtmann, S. Rajagopalan, C.C. Winter, M. Peruzzi, E.O. Long, Killer cell inhibitory receptors specific for HLA-C and HLA-B identified by direct binding and by functional transfer, Immunity 3 (1995) 801–809.

[10] K. Maenaka, T. Juji, T. Nakayama, J.R. Wyer, G.F. Gao, T. Maenaka, N.R. Zaccai, A. Kikuchi, T. Yabe, K. Tokunaga, K. Tadokoro, D.I. Stuart, E.Y. Jones, P.A. Van der Merwe, Killer cell immunoglobulin receptors and T cell receptors bind peptide-major histocompatibility complex class I with distinct thermodynamic and kinetic properties, J. Biol. Chem. 274 (1999) 28329–28334.

[11] M. Carrington, M.P. Martin, The impact of variation at the KIR gene cluster on human disease, Curr. Top. Microbiol. Immunol. 298 (2006) 225–257.

[12] N. Tsuchiya, C. Kyogoku, R. Miyashita, K. Kuroki, Diversity of human immune system multigene families and its implication in the genetic background of rheumatic diseases, Curr. Med. Chem. 14 (2007) 431–439.

[13] E.Y. Park, M. Ishikiriyama, T. Nishina, T. Kato, H. Yagi, K. Kato, H. Ueda, Human IgG1 expression in silkworm larval hemolymph using BmNPV bacmids and its N-linked glycan structure, J. Biotechnol. 139 (2009) 108–114.

[14] H. Nakagawa, Y. Kawamura, K. Kato, I. Shimada, Y. Arata, N. Takahashi, Identification of neutral and sialyl N-linked oligosaccharide structures from human serum glycoproteins using three kinds of high-performance liquid chromatography, Anal. Biochem. 226 (1995) 130–138.

[15] N. Takahashi, H. Nakagawa, K. Fujikawa, Y. Kawamura, N. Tomiya, Three-dimensional elution mapping of pyridylaminated N-linked neutral and sialyl oligosaccharides, Anal. Biochem. 226 (1995) 139–146.

[16] H. Yagi, N. Takahashi, Y. Yamaguchi, N. Kimura, K. Uchimura, R. Kannagi, K. Kato, Development of structural analysis of sulfated *N*-glycans by multidimensional high performance liquid chromatography mapping methods, Glycobiology 15 (2005) 1051–1060.

[17] N. Takahashi, K. Kato, GALAXY (glycoanalysis by the three axes of MS and chromatography): a web application that assists structural analysis of *N*-glycans, Trends Glycosci. Glycotech. 15 (2003) 235–251.

[18] Q.R. Fan, L. Mosyak, D.N. Garboczi, C.C. Winter, N. Wagtmann, E.O. Long, D.C. Wiley, Structure of a human natural killer cell inhibitory receptor, Transplant. Proc. 31 (1999) 1871–1872.

[19] R. Misaki, H. Nagaya, K. Fujiyama, I. Yanagihara, T. Honda, T. Seki, N-linked glycan structures of mouse interferon-beta produced by *Bombyx mori* larvae, Biochem. Biophys. Res. Commun. 311 (2003) 979–986.

[20] S. Watanabe, T. Kokuho, H. Takahashi, M. Takahashi, T. Kubota, S. Inumaru, Sialylation of *N*-glycans on the recombinant proteins expressed by a baculovirus-insect cell system under beta-*N*-acetylglucosaminidase inhibition, J. Biol. Chem. 277 (2002) 5090–5093.

Please cite this article in press as: K. Sasaki et al., Silkworm expression and sugar profiling of human immune cell surface receptor, KIR2DL1, Biochem. Biophys. Res. Commun. (2009), doi:10.1016/j.bbrc.2009.07.065

Mod Rheumatol (2009) 19:293–301
DOI 10.1007/s10165-009-0154-4

ORIGINAL ARTICLE

Time of initial appearance of renal symptoms in the course of systemic lupus erythematosus as a prognostic factor for lupus nephritis

Yuko Takahashi · Tetsuya Mizoue · Akitake Suzuki · Hiroyuki Yamashita · Junwa Kunimatsu · Kenji Itoh · Akio Mimori

Received: 31 October 2008 / Accepted: 19 January 2009 / Published online: 10 March 2009

Abstract The prognosis of lupus nephritis (LN) was studied retrospectively in two LN categories, LN manifested initially at systemic lupus erythematosus (SLE) onset (I-LN) and LN of delayed manifestation after SLE onset (D-LN), based on a chart review (C) of 154 SLE (85 LN) patients with a mean observation of 20.8 ± 9.3 years and a questionnaire study (Q) of 125 LN patients outside our hospital with mean observation of 17.6 ± 9.2 years. In both study groups, half of I-LN patients were relapse-free by Kaplan–Meier analysis after initial therapy, and the relapsed I-LN patients responded to retherapy at higher 5-year relapse-free rates than those of patients receiving initial therapies for D-LN. At last observation, a higher frequency of prolonged remission was shown in I-LN compared with D-LN patients (C: 22/31, 71% versus 14/49, 29%, $P < 0.01$; Q: 65/89, 73% versus 11/33, 33% $P < 0.01$) and also a higher frequency of irreversible renal damage in D-LN compared with I-LN patients (C: 25/49, 51% versus 2/31, 6%, $P < 0.001$; Q: 14/33, 42% versus 6/89, 7%, $P < 0.001$), although class IV pathology was common in patients (C) in both LN categories. Onset time of lupus nephritis in the course of SLE may affect renal prognosis.

Y. Takahashi · A. Suzuki · H. Yamashita · J. Kunimatsu · K. Itoh · A. Mimori (✉)
Division of Rheumatic Diseases,
International Medical Center of Japan,
1-21-1 Toyama, Shinjuku-ku, Tokyo 162-8655, Japan
e-mail: amimori@imcj.hosp.go.jp

T. Mizoue
Department of Epidemiology and International Health,
Research Institute, International Medical Center of Japan,
1-21-1 Toyama, Shinjuku-ku, Tokyo 162-8655, Japan

Keywords Lupus nephritis · Onset · Prognosis · SLE

Introduction

Systemic lupus erythematosus (SLE) is a multiple-organ disease, and lupus nephritis (LN) is a major clinical problem because of its high morbidity and mortality rates. In accordance with the chronic nature of SLE, renal symptoms can manifest at various times in the disease course, and a physician cannot predict the future development of LN at the time of SLE onset. Furthermore, it is unclear whether there is a difference in prognosis between LN manifested at the onset of SLE and LN developed later in the course of SLE, because the clinical significance of time of LN onset in the disease course of SLE has not been clearly described in the literature, to our knowledge. Accordingly, in recent clinical trials on therapies for LN including cyclophosphamide and mycophenolate mofetil, mixtures of cases having various time intervals between SLE onset and LN onset have been studied [1, 2]. Although a prognostic impact of renal pathology and a poor prognosis of class IV disease have been established in LN based on the World Health Organization (WHO) classification [3–5] and more recent criteria [3, 6, 7], a later progression or transformation of the pathology cannot necessarily be predicted at the time of the initial biopsy [8, 9].

In our preliminary chart review, we found that numerous cases of remitted SLE had class IV LN at SLE onset. On the other hand, irreversible renal damage was precipitated in patients who initially showed no renal symptoms but later developed LN with various renal pathologies, and the LN of later development was never a case of senile-onset LN. Thus we undertook to study the possible relationship

between renal prognosis and the time of the initial renal manifestation in the course of SLE. The study consisted of two parts: a chart review in our institute and a replication study to reconfirm the results of the chart review using a questionnaire administered to LN patients outside our hospital.

Patients and methods

Chart review for patients with SLE

Hospital records of the International Medical Center of Japan were reviewed for patients with SLE having a disease duration of 5 years or more. SLE was diagnosed according to the classification criteria of the American College of Rheumatology [10]. The clinical information on 154 patients with SLE (139 females and 15 males) with mean age of 48.9 ± 12.6 (median 48) years at the last observation was available for studying the entire disease course, including 436 major therapeutic interventions for SLE and 22 deaths during 3,189 person-years or mean observation period of 20.7 ± 9.3 years. At the time of the present study, 85 patients (80 females and 5 males) had LN, and 28 of these had irreversible renal dysfunction, including 15 patients on hemodialysis therapy.

Onset age, relapse ages, therapeutic doses if available, renal pathology data if any, and disease status after therapy and at the last observation in each patient were serially input in our database for SLE patients. The definition of relapse will be provided in "Results". Minor dose increases during steroid therapy for mild activities of SLE were not analyzed. Chronological profiles of the onsets and relapses of LN or extrarenal SLE flares were analyzed statistically with Stata 9.0 (Stata Corp., College Station, TX, USA).

Questionnaire study for patients with LN

To reconfirm the results of the chart review study in another LN patient group, we undertook a questionnaire study of SLE patients outside our hospital and collected individual data on LN with a SLE duration of 5 years or more. The questionnaire included ages at all of the hospitalizations due to SLE and/or LN from onset to the present time, daily doses of steroid (number of 5 mg prednisolone tablets) before and at the start of therapeutic interventions, combined use of intravenous pulse steroid or cyclophosphamide, and renal status at each hospitalization and at the present time. Renal status, which was based on the information from an attendant doctor to each patient, was expressed in terms of urine protein (negative, positive, nephrotic, or 1+ to 4+), data of serum creatinine levels if available, and clinical categories including no abnormalities, mild persistent renal disease, nephrotic syndrome, renal dysfunction or on hemodialysis.

The ethics committee of our hospital approved the present study. A questionnaire sheet including a description of the aim of our study was inserted once in the *Journal of Patients' Association of Collagen Diseases* in Japan, which was subscribed to by more than 5,000 patients, including approximately 3,000 patients with SLE. An anonymous letter in reply (datasheet) sent to the board of the above Patients' Association with a completed questionnaire was regarded as informed consent to enter the present study. We received a set of the copied datasheets from the board, which preserved the original sheets.

After removing approximately 50 cases with insufficient information in the datasheets, 7 cases having SLE without LN, and 10 cases of SLE with less than 5 years' duration, we recognized 125 datasheets that contained a sufficient description of LN. The filling of a datasheet and voluntary mailing might have resulted in a strong bias toward selecting informative repliers from among thousands of patients. The 125 patients were characterized by excellent medical compliance and were thought to have preserved written records on their own diseases.

The studied patients

Mean age of the 125 patients (121 females and 4 males) in the present study was 46.5 ± 12.5 years (median 46 years). A total of 331 hospitalizations because of therapy for SLE were mentioned during 2,200 person-years, or mean observation period of 17.6 ± 9.2 years. Chronological profiles of the relapses of LN were analyzed statistically with Stata 9.0 similarly to the analysis of the chart review study. Renal pathology in accordance with the WHO classification was mentioned in only 19 datasheets and was not analyzed.

In our SLE database, a whole chronological profile of each patient including all of the hospitalizations from onset to the last observation was specific to one subject like a fingerprint, and no overlapping cases were found by computer analysis.

Results

Definitions of initial-onset LN and delayed-onset LN in the course of SLE

In both the chart review and the questionnaire study, some of the patients had been observed with no or low-dose steroid therapy for their mild SLE conditions during the early disease course, and the initial urine proteins were documented

as negative in most of these patients or unknown in some of the referral patients, except in a small number of patients who received no therapy for their positive renal symptoms.

In the present study, we defined a SLE relapse as hospitalization in order to treat SLE after previous SLE conditions have subsided in response to treatment during hospitalization. In a small number of cases, initial steroid therapy with 20 mg/day or more of prednisolone equivalent was started at an outpatient clinic, and we classified the therapy as "treatment under hospitalization" for simplicity in the present text. We further defined "initial-onset LN" and "delayed-onset LN" as follows.

Initial-onset LN (I-LN)

I-LN was defined as LN diagnosed at the time of onset of SLE, LN diagnosed at the initial treatment under hospitalization for SLE or LN that emerged during the initial course of therapy under hospitalization. Two of the 34 I-LN patients in the chart review and 7 of the 91 I-LN patients in the questionnaire study met one of the latter two definitions of I-LN.

Delayed-onset LN (D-LN)

D-LN was defined as newly developed LN as a SLE relapse after the previous successful therapy under hospitalization. At the time of the present study, 51 patients in the chart review and 34 patients in the questionnaire study were classified into this category of LN.

Mean ages of the patients at SLE onset and D-LN onset in the present study are shown in Table 1. These data were very similar between the two study groups; the mean interval between SLE onset and D-LN onset was approximately 8.9 years in the chart review and 7.3 years in the questionnaire study.

Time course of D-LN developments in the chart review patients is shown in Fig. 1a. The Kaplan–Meier curve showed that D-LN developed in half of the SLE patients of extrarenal onset, and that half of the instances of D-LN occurred after 10 disease-years of SLE. We note that the curve might not represent a natural course of D-LN development among SLE patients because of possible sampling bias by the chart review in our single institute and based on our knowledge of the widely different frequencies of LN among SLE patients noted in the literature [11]. A comparable analysis could not be performed in the questionnaire study, because we collected only cases with a positive history of LN.

Time course of the first-time relapse of SLE after the initial treatment under hospitalization in the chart review patients (Fig. 1b)

A total of 302 SLE relapses were identified in the 154 chart review patients, and these included 110 renal involvements and 192 extrarenal SLE flares. The patients were classified into one of two groups, I-LN ($n = 34$) and others ($n = 120$), at the start point of the analysis. Patients in the "others" group, in whom LN developed later, were further classified into D-LN ($n = 51$), as defined above.

The Kaplan–Meier curve indicating those free from SLE relapse after the initial treatment under hospitalization showed a longer relapse-free period in the I-LN patients compared with the other patients (12 versus 4 years to the first relapse was expected in 50% of each patient group, $P = 0.008$) (Fig. 1b), when patients who received no or low-dose steroid were removed from the analysis.

Most of the patients without I-LN had mild SLE conditions at the time of the initial treatment under hospitalization, because neuropsychiatric involvement was not common as the initial manifestation (data not shown).

Table 1 Onset age and initial therapy for LN and/or SLE

		Onset age, years (mean ± SD)	Dose of therapy (PSL[a], mg/day)	Patient ratio that received pulse steroid[b] or IVCY[c]	
Chart review ($n = 85$)					
I-LN ($n = 34$)	SLE + LN	29.1 ± 14.8	51.3 ± 15.2 ($n = 31$)	26% (8/31)	10% (3/31)
D-LN ($n = 51$)	SLE	25.0 ± 10.9	35.0 ± 13.1 ($n = 42$)	#	
	LN	33.9 ± 12.2	41.3 ± 14.4 ($n = 45$)	64% (29/45)	2% (1/45)
Questionnaire study ($n = 125$)					
I-LN ($n = 91$)	SLE + LN	30.1 ± 12.1	44.7 ± 14.7 ($n = 84$)	29% (26/91)	12% (11/91)
D-LN ($n = 34$)	SLE	27.1 ± 11.8	39.1 ± 16.7 ($n = 32$)	#	
	LN	34.4 ± 13.5	43.0 ± 15.2 ($n = 27$)	32% (11/34)	15% (5/34)

[a] PSL, prednisolone equivalent

[b] Intravenous methylprednisolone pulse therapy

[c] Intravenous cyclophosphamide pulse therapy

Pulse steroid or IVCY was rarely used for SLE of D-LN patients at the onset of SLE

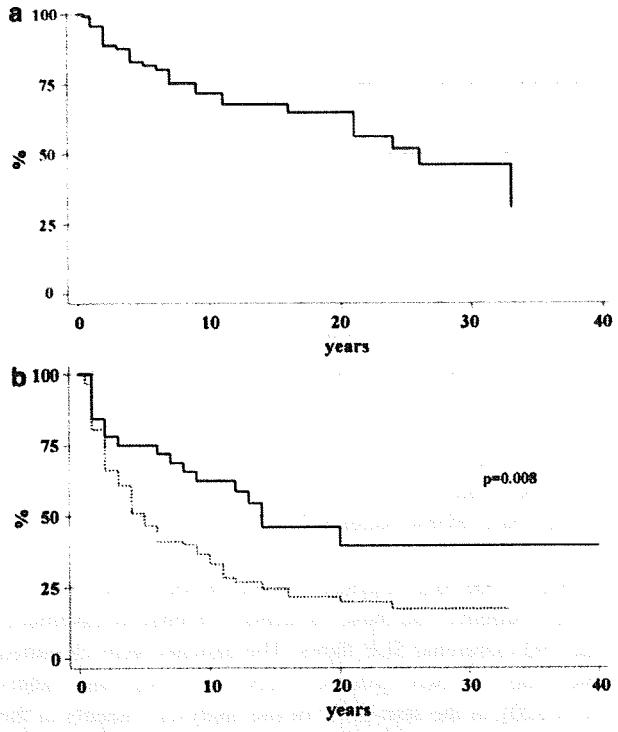

Fig. 1 **a** Kaplan–Meier curve indicating those free from LN development, for patients without initial renal involvement at onset of SLE in the chart review study. Analysis starts at the onset of SLE, and the result shows a time course of developing delayed-onset LN (D-LN). **b** Kaplan–Meier curve indicating those free from SLE relapse after the initial therapy for SLE in the chart review study. Analysis starts at the initial treatment under hospitalization for SLE. *Solid line* patients in whom the initial therapy was targeted at LN (I-LN) ($n = 31$). *Dotted line* patients in whom the initial therapy was targeted at SLE without renal involvement ($n = 95$). The log-rank test was used for statistical analysis

Accordingly, the mean initial steroid dose tended to be higher in the I-LN patients (prednisolone equivalent: 51.3 ± 15.2 mg/day, $n = 31$ versus 36.4 ± 14.1 mg/day, $n = 52$ in the non-I-LN patients of identified steroid dose). High-dose pulse steroid or cyclophosphamide was combined in a quarter of or a small number of I-LN patients (Table 1), respectively, for treating the LN, and was rarely used in non-I-LN patients. Because I-LN and non-I-LN have different organ involvement, the difference in relapse rates after therapy between the two disease categories may not be attributed to the difference in therapeutic intensities. If renal involvement at the onset of SLE indicates a severe form of SLE, a longer relapse-free period in the I-LN patients than in the non-I-LN patients (Fig. 1b) may be paradoxical, or it may be attributed to D-LN development in the non-I-LN patients. Thus, we further studied therapeutic responses in the I-LN patients and the D-LN patients.

Renal relapse-free rates in the I-LN patients (Fig. 2)

The Kaplan–Meier curve indicating freedom from LN relapse after the initial treatment under hospitalization for the I-LN is shown in Fig. 2 for the chart review patients and the questionnaire study patients. A total of five patients who received no therapeutic intervention for LN were removed from the calculation. The results in the two study groups showed consistently that half of the I-LN patients were expected to be renal-relapse-free after the initial therapy.

In the chart review, 18 (58%) of 31 treated patients had no LN relapse throughout the observation period, and all of these patients achieved complete renal remission, although extrarenal SLE flares were observed in 5 patients. Renal relapse was defined as rehospitalization in order to treat SLE accompanied by emerging or increasing proteinuria. Renal remission was defined by normal serum creatinine levels and no urine abnormalities

In the questionnaire study, 52 (58%) out of 89 treated patients had no LN relapse throughout the observation. Of these, 90% (47/52) of the patients achieved complete renal

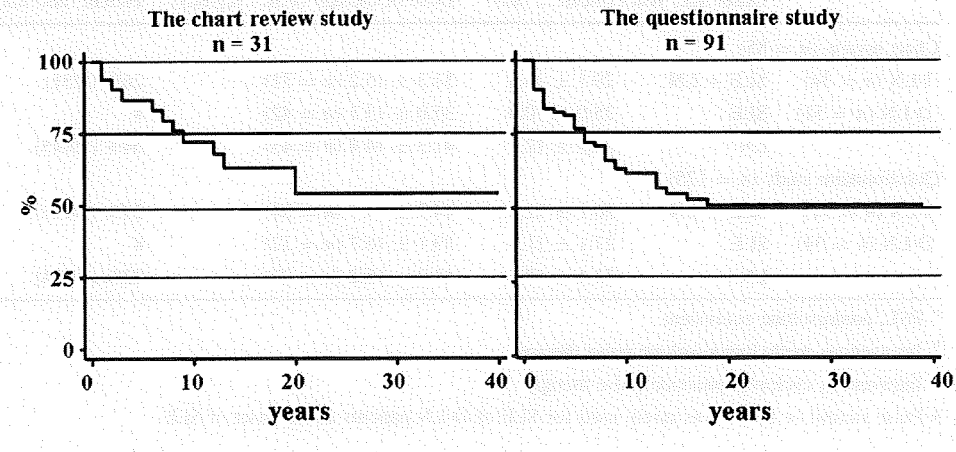

Fig. 2 Kaplan–Meier curve indicating patients free from LN relapse after the initial therapy for I-LN in the two study groups. Analysis starts at the initial treatment under hospitalization for I-LN

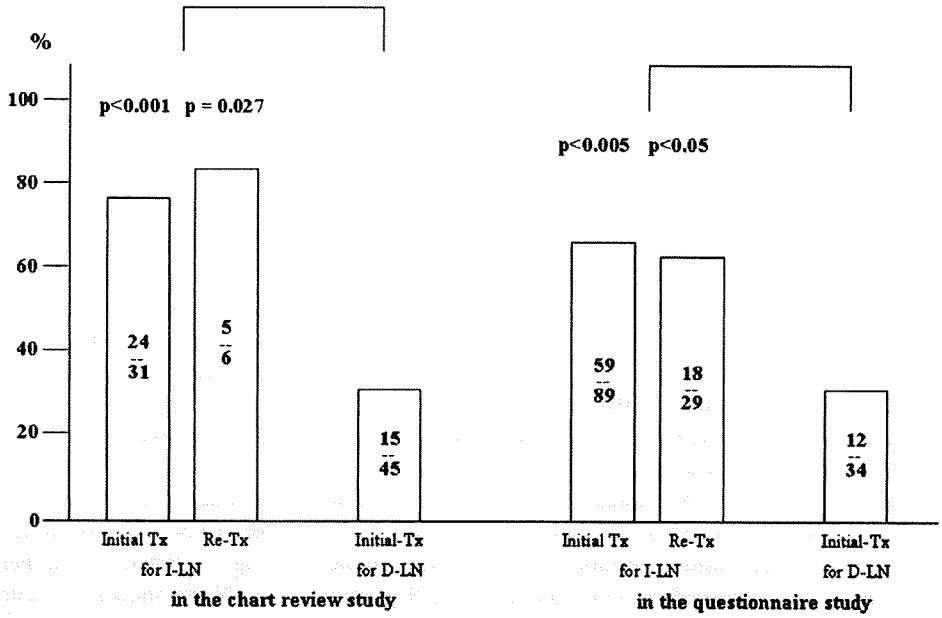

Fig. 3 Response rate to therapy for LN. Initial therapy for I-LN, retherapy for relapsed I-LN, and initial therapy for D-LN were studied by historical follow-up for 5 years; ratios of patients who responded to therapy for LN are shown. Definition of therapeutic response is given in the text. Chi-squared or Fisher's exact probability test was used for statistical analysis

remission. Of the remaining five patients with no relapse but no remission, three patients had massive urine protein and elevated serum creatinine levels at SLE onset that did not respond to initial therapies, and renal deterioration progressed without further therapeutic interventions, and the other two patients had mild persistent urine protein at the last observations.

These results regarding renal relapse suggested that renal remission was common in I-LN only in response to the initial therapy. We further studied prognoses of relapsed I-LN patients in comparison with those of D-LN patients, because first-time relapse of I-LN and onset of D-LN are similarly defined under "relapse of SLE."

Comparison of renal response to therapy between I-LN and D-LN (Fig. 3)

Initial therapies for I-LN or D-LN, respectively, were begun based on renal biopsy in most of the patients of the chart review study, as described later, and positive urine protein was found to be a major reason for the therapeutic intervention in all of the chart review and the questionnaire study patients. Retherapy for relapsed I-LN was begun at the time of rehospitalization in order to treat SLE accompanied by emerging or increasing proteinuria.

Response criteria

Responses to therapy for LN were estimated by 5-year historical follow-up after the initial therapy for I-LN or D-LN, and after the retherapy for I-LN of the first-time relapse. Positive renal response was defined as no relapse, no progressive renal dysfunction, and no nephrotic levels of urine protein during 5-year observation after therapy. The patients in the chart review study who responded to therapy also met response criteria similar to those in the literature [12], i.e., serum creatinine not exceeding the lowest level during treatment under hospitalization, proteinuria less than 3+ or a urine-protein/creatinine ratio less than 1, and no nephritic findings in the urine sediment for at least 6 months after therapy. In the questionnaire study patients, the responses to therapy were identified based on the mention of no renal dysfunction and no or less than 3+ proteinuria after therapy.

Patients who received no therapeutic intervention for renal deterioration were removed from the calculation. In the descriptions below, we classified a patient who showed both renal abnormalities and renal relapse after therapy into a category of renal relapse.

Chart review study

A better renal response to initial therapy was observed in the I-LN patients compared with the D-LN patients (Fig. 3). Initial steroid therapies for LN in the I-LN and the D-LN are shown in Table 1. The difference in the therapeutic doses did not seem large enough to explain the different response rates between the I-LN and the D-LN patients.

WHO class IV histology was documented at the renal biopsy before therapy for LN with similar frequencies (I-LN: 14/21, 64% versus D-LN: 22/39, 56%) in the two LN categories, and the chronic lesions were each identified in only a small number of patients. The total results of

histology identified in 21 I-LN versus 39 D-LN were: II, 1 versus 5; III, 0 versus 1; IVa or b, 6 versus 10; IVc, 2 versus 4; IVd, 0 versus 0; IV of unknown subclass, 6 versus 8; V, 6 versus 11; and there was no significant difference in the distribution of the histology between I-LN and D-LN.

Serological data before therapy (the number of patients) were identified in most of the patients treated for I-LN (31) or D-LN (45). Serum anti-DNA antibody levels were elevated in 89% (24/27) of I-LN patients and 93% (37/40) of D-LN patients; the mean titer in I-LN patients was 100.5 ± 20.1 IU/ml ($n = 11$) by enzyme-linked immunosorbent assay (ELISA) for anti-double-stranded DNA IgG antibodies (normal range <20), 10 ± 2 IU/ml ($n = 10$) by radioimmunoassay (RIA) for anti-DNA antibodies (normal range <6), or unknown except positive results ($n = 3$), whereas that in D-LN patients was 56.7 ± 11.2 IU/ml ($n = 12$) by ELISA, 12 ± 2 IU/ml ($n = 15$) by RIA, or unknown except positive results ($n = 10$). Hypocomplementemia was observed in 83% (20/24) of I-LN patients and 93% (38/41) of D-LN patients based on the data of serum C3 and/or CH50. Of these, the comparable assays for C3 (normal range 60–95 mg/dl) showed mean levels 40.2 ± 5.6 mg/dl ($n = 13$) in I-LN patients and 43.5 ± 9.9 mg/dl ($n = 27$) in D-LN patients, respectively. The above data showed that the two patient groups I-LN and D-LN had similar serological abnormalities before initial therapy for LN.

Renal status (number of patients) during 5 years after initial therapy for LN

The 31 I-LN patients showed one of the following: 5-year remission (22), mild persistent proteinuria (2) including accompanied renal dysfunction (1) with serum creatinine >1 mg/dl after rapidly progressing glomerulonephritis (RPGN), or renal relapse (6). A negative response was found in seven patients.

The 45 D-LN patients showed one of the following: 5-year remission (10), mild persistent proteinuria (5), or persistent proteinuria of nephrotic levels (5), including accompanying renal dysfunction (3) with serum creatinine >1 mg/dl after RPGN, or renal relapse (25). A negative response was found in 30 patients.

Renal status during 5 years after retherapy for the first relapse of I-LN

LN relapse occurred in 11 of the 31 I-LN patients after the initial therapy. Of these, nine patients received therapeutic interventions at the mean prednisolone-equivalent dose of 44.4 ± 15.1 mg/day, and a methylprednisolone pulse was added in two patients. By the time of the present study, six patients had been followed for more than 5 years after the retherapy for LN; 5-year remission (three), mild persistent proteinuria (two) or a second renal relapse (one) during 5 years were found in the six patients. A negative response was found in one patient. The renal response to the retherapy was again better than that following the initial therapy for D-LN (Fig. 3).

Serum anti-DNA antibody levels before therapy were elevated in 89% (8/9) of the patients treated for relapsed I-LN, and the mean titer was 59.5 ± 22.1 IU/ml ($n = 5$) by ELISA or 8 ± 2 IU/ml ($n = 3$) by RIA. Hypocomplementemia was observed in 78% (7/9) of the patients, and the mean serum C3 level was 48.1 ± 5.1 mg/dl ($n = 7$).

The questionnaire study

A better renal response to initial therapy was observed in the I-LN patients compared with the D-LN patients (Fig. 3). Initial steroid therapies for LN in the I-LN and the D-LN are shown in Table 1. The difference in the therapeutic doses did not seem large enough to explain the different response rates between the I-LN and the D-LN patients.

Renal status (the number of patients) during 5 years after initial therapy for LN

The 89 I-LN patients showed one of the following: 5-year remission (32), probable remission or mild proteinuria (16), mild persistent proteinuria (11), chronic proteinuria of nephrotic levels accompanying renal dysfunction (3) after RPGN, or renal relapse (27). "Probable remission or mild proteinuria" was defined based on no subsequent relapse and the mention of no renal abnormalities at the last observation but no mention of the early renal status after therapy. A negative response was found in 30 patients.

The 34 D-LN patients showed one of the following: 5-year remission (9), mild persistent proteinuria (3), persistent proteinuria of nephrotic levels and/or renal dysfunction (12), or renal relapse (10). At least five patients had RPGN before therapy. A negative response was found in 22 patients.

Renal status during 5 years after retherapy for the first relapse of I-LN

LN relapse occurred in 39 of the 91 I-LN patients, and 36 patients received therapeutic interventions. The identified mean prednisolone-equivalent dose was 45.5 ± 13.3 mg/day ($n = 30$), and the combination use of steroid pulse was mentioned by ten patients, and that of cyclophosphamide by six patients. The 29 patients who received retherapy and 5-year follow-up showed one of the following: 5-year remission (8), mild persistent proteinuria

Table 2 Renal outcomes of I-LN or D-LN in the two study groups: renal status over 3 years at time of the last observation

	n	Remission	MPD	N + CRF + HD	Flare	Observation period of LN (years)
Chart review						
I-LN	31	22 (71%)*	7	0 + 0 + 2 (6%)	0	19.6 ± 9.2
D-LN	49	14 (29%)	8	4 + 11 + 10 (51%)**	2	13.0 ± 8.1
Questionnaire study						
I-LN	89	65 (73%)*	8	0 + 4 + 2 (7%)	10	17.5 ± 9.1
D-LN	33	11 (33%)	5	6 + 4 + 4 (42%)**	3	12.1 ± 7.8

Remission: no renal abnormalities but including SLE conditions of serologically active clinically quiescent (SACQ) disease for at least 3 years. MPD (mild persistent disease; positive urine proteins less than nephrotic levels). N (nephrotic levels of urine proteins): prolonged massive urine proteins without apparent renal dysfunction. CRF (chronic renal failure but no uremia): prolonged elevation of serum creatinine levels (>1 mg/dl) or mention of renal dysfunction in the questionnaire based on information from attendant doctors. HD (hemodialysis): on maintenance HD or having a history of receiving renal implantation irrelevant to the present renal status. Flare: flare of SLE and/or LN within 3 years by the last observation

* $P < 0.01$, ** $P < 0.001$ (chi-squared test)

(3), probable remission or mild proteinuria (7), persistent proteinuria of nephrotic levels and/or renal dysfunction (2), or a second renal relapse (9). A negative response was found in 11 patients. The renal response to the retherapy was again better than that following the initial therapy for D-LN (Fig. 3).

The results in the two study groups were consistent, and suggested that renal response to both the initial therapy for I-LN and the retherapy for relapsed I-LN were better than that to the initial therapy for D-LN.

Renal outcomes: renal status over 3 years at the time of the last observation (Table 2)

Renal status was classified according to definitions described in the footnotes of Table 2, and we classified a patient that showed both of chronic renal damage and recent renal flare into a category of chronic renal damage but not flare. A higher frequency of renal remission was observed in I-LN compared with D-LN, and a higher frequency of irreversible renal damage including nephrotic levels of prolonged urine proteins or chronic renal failure was observed in D-LN compared with I-LN.

The above results were consistent in the two study groups and suggested a good renal prognosis of I-LN patients and a poor renal prognosis of D-LN patients. In most of the patients with irreversible renal damage in the present study, frequent relapse resulted in renal deterioration.

Patients whose irreversible renal damage was established before the initial therapy were removed from the estimation of renal outcomes shown in Table 2. This included three I-LN patients and two D-LN patients in the chart review and two I-LN patients and one D-LN patient in the questionnaire study. Some of the remaining patients in the chart review did not receive an appropriate therapeutic intervention for renal deterioration that developed in the course of SLE for various reasons, including a referral delay, poor medical compliance, and accompanying chronic infection.

Except in the case of receiving insufficient therapy as described above, most of the patients in the chart review and the questionnaire study were treated for LN appropriately with 30–60 mg/day prednisolone-equivalent doses of steroid at the onset of LN and at the first LN relapse. For repeated SLE relapses, however, intensities of therapeutic interventions were widely different from case to case.

Renal outcomes in reference to the renal pathology before therapy in the chart review study

Renal pathology before initial therapy for LN (the first-time biopsy; Fig. 4)

Renal outcomes in the chart review patients were collated according to the renal pathology data at biopsy before initial therapy (Fig. 4), which were available in 61 out of 85 LN patients based on the reports by pathologists in our hospital or the referral description of other hospitals. In addition, one I-LN and three D-LN patients manifested RPGN at the onset of LN and had probable class IV-LN.

The descriptions of renal pathology found by chart review were mostly in accordance with the WHO classification (3, 4), although the information on subclass was not comprehensive. In the present study (Fig. 4), we classified "a description of membranous LN" or "class V without description of combined III or IV" into "V", and "diffuse proliferative LN without subclass-description" into "IV-" (Fig. 4). In addition, "IV + V" documented in some of the case records was also denoted as "IV-" but not Vd. Thus, "IV-" in Fig. 4 might contain various types of class IV.